USE OF THE WAVE EQUATION TO PREDICT SOIL RESISTANCE ON A PILE DURING DRIVING

by
Lee L. Lowery, Jr.
Assistant Research Engineer
Thomas C. Edwards
Assistant Research Engineer
and
T. J. Hirsch
Research Engineer

Research Report 33-10

Piling Behavior
Research Study 2-5-62-33

Sponsored by
The Texas Highway Department

In cooperation with the
U. S. Department of Transportation
Federal Highway Administration
Bureau of Public Roads

August 1968

TEXAS TRANSPORTATION INSTITUTE
Texas A&M University
College Station, Texas

FOREWORD

The information contained herein was developed on Research Study 2-5-62-33 entitled "Piling Behavior" which is a cooperative research study sponsored jointly by the Texas Highway Department and the U. S. Department of Transportation, Federal Highway Administration, Bureau of Public Roads. The broad objective of this study is to fully develop the use of the computer solution of the wave equation so that it may be used to predict driving stresses in piling and to estimate static load bearing capacity of piling.

This report concerns itself with the latter objective of estimating static load bearing capacity of piling. This paper describes how the wave equation can be used to estimate the soil resistance acting on a pile at the time of driving. Knowing the soil resistance on the pile at the time of driving, one can then estimate the load bearing capacity by considering the time effect or soil "set-up" which tends to increase the pile bearing capacity. This report compares the wave equation predictions with full-scale pile load tests results which were conducted by the Texas Highway Department, United States Corps of Engineers, and the Michigan Highway Department.

The opinions, findings, and conclusions expressed in this report are those of the authors and not necessarily those of the Bureau of Public Roads.

ACKNOWLEDGMENTS

During the course of this study, many individuals provided cooperation and support. Acknowledgment is due Mr. Clifford B. Rouse, Senior Resident Engineer, and Mr. Gerald R. Scalf, Senior Resident Engineer, both of District 16 of the Texas Highway Department, for their cooperation in the field tests conducted at Copano Bay.

Special thanks go to Mr. Albert C. Frankson, Senior Resident Engineer, and Patrick H. Keefe, Jr., Senior Resident Engineer, both of District 13, for their cooperation and assistance in the conduct of the field tests conducted in Victoria.

Special gratitude is expressed also to Mr. George P. Munson, Jr., Assistant District Engineer, and Mr. Francis G. Miksovsky, Senior Resident Engineer, both of District 12 of the Texas Highway Department, for their assistance and cooperation in conducting the field tests at Chocolate Bayou.

The assistance of Mr. William B. Ward, Urban Designing Engineer of the Houston urban project of the Texas Highway Department, in conducting the pile tests in Houston is gratefully acknowledged.

The assistance and cooperation of all the personnel of the Texas Highway Department, too numerous to name, is appreciated. Without the help of these dedicated employees of the state the research reported herein would not have been possible.

Recognition is also due Mr. Farland C. Bundy, Supervising Design Engineer, Mr. Horace E. Hoy, Senior Soils Engineer, and Mr. Wayne Henneberger, Engineer of Bridge Design, all of the Bridge Division of the Texas Highway Department, for their cooperation in carrying out this study.

The following employees of the Texas Transportation Institute are recognized for their contribution to this report: Mr. Gene Weiderhold for his assistance in the preparation and installation of instrumentation and the conduct of field tests; and Mr. Bob Whitson for helping in the reduction of data from the field tests.

TABLE OF CONTENTS

LIST OF FIGURES

LIST OF TABLES

Use of the Wave Equation to Predict Soil Resistance On a Pile During Driving

Chapter I

INTRODUCTION

The study of behavior of piling has received considerable attention by investigators in the past. Much work has been directed toward establishing simplified formulas, both empirical and semirational, for predicting ultimate load bearing capacity from a pile's driving resistance (permanent set per blow).

It is generally recognized that none of the simplified formulas have proven completely satisfactory for the broad spectrum of pile types, pile drivers, and soil conditions encountered in present-day foundation problems. For a discussion of pile formulas, the reader is referred to the work of Chellis (1)*.

Previous papers by the Institute have dealt with using the wave theory in the structural analysis of piling (computing driving stresses and effects of different cushions and driving equipment). The purpose of this report is to show how Smith's pile driving analysis (3) by the wave equation can be used to predict the soil resistance on a pile at the time of driving.

*Numerals in parentheses refer to corresponding items in the Reference list.

Chapter II

BRIEF DESCRIPTION OF PILE DRIVING ANALYSIS BY THE WAVE EQUATION

The Wave Equation

In 1940, Cummings (2) discussed dynamic pile-driving formulas in general and provided a brief description of the wave-theory approach and the theoretical work of Glanville and his associates.

The work of Smith in adapting wave theory in a more realistic manner to the actual conditions met in pile driving is given in detail in Reference (3). Smith published considerable previous work (4), (5), (6) leading to the development of his procedure.*

The wave-theory approach to the problem does not involve a "formula" in the usual sense. The basis for the procedure is the classical one-dimensional wave equation.

$$\frac{\partial u^2}{\partial t^2} = c^2 \frac{\partial u^2}{\partial x^2} \qquad (1)$$

where

- c = velocity of propagation of longitudinal strain wave along bar $= \sqrt{E/\rho}$,
- x = direction of longitudinal axis,
- u = displacement of bar cross section in x direction,
- t = time, and
- E = modulus of elasticity
- ρ = mass per unit volume of material.

*For a more comprehensive description of pile driving analysis by the wave equation, see references (7) and (8).

Smith's Idealization

Fig. 2.1 illustrates the idealization of the pile system suggested by Smith. In general, as seen in Fig. 2.1 (a), the system is considered to be composed of:

1. a ram, to which an initial velocity is imparted by the pile driver,
2. a capblock (cushioning material),
3. a pile cap,
4. a cushion block (cushioning material),
5. a pile, and
6. the supporting medium, or soil.

In Fig. 2.1 (b) the idealizations for the various components of the actual pile are shown. The ram, capblock, pile cap, cushion block, and pile are pictured as appropriate discrete weights and springs. The frictional soil resistance on the side of the pile is represented by a system composed of springs and dashpots; the point soil resistance is accounted for by a single spring and dashpot at the point. The characteristics of these various components will be discussed later.

Actual situations may deviate from that in Fig. 2.1. For example, a cushion block may not be used or an anvil may be placed between the ram and capblock. Such cases are readily accommodated.

Internal Springs

The ram, capblock, pile cap, and cushion block may in general be considered to consist of "internal springs,"

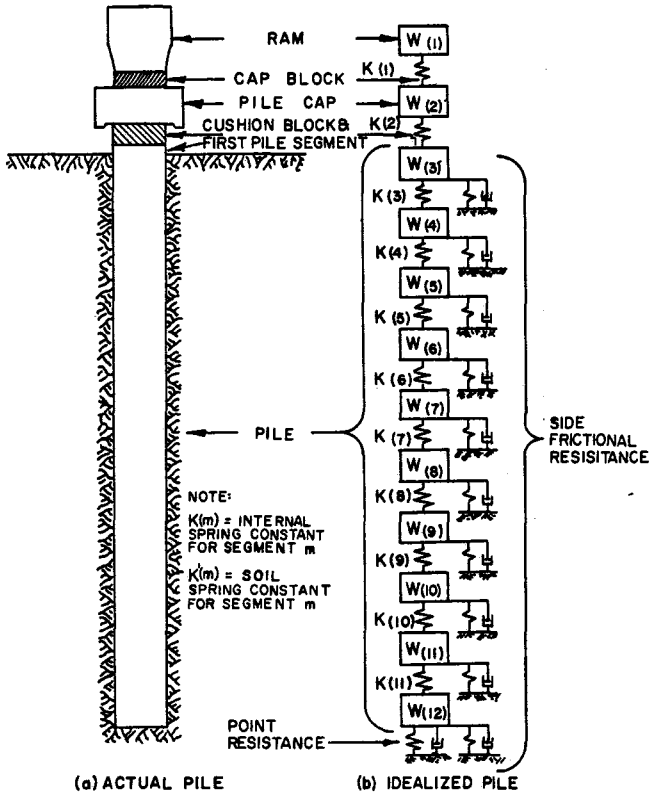

Fig. 2.1. Idealization of a pile for purpose of analysis.

although in the representation of Fig. 2.1 (b) the ram and the pile cap are treated as rigid bodies (a reasonable assumption for many practical cases). In Fig. 2.2(a), the pile material is considered to experience no internal damping. In Fig. 2.2(b), the capblock and cushion block material is assumed to exhibit internal damping according to the linear relationships shown.

External Springs

The resistance to dynamic loading afforded by the soil in shear along the outer surface of the pile and in bearing at the point of the pile is not clearly understood. These resistances are under study in another phase of this project. Fig. 2.3(a) shows the load-deformation characteristics assumed for the soil in Smith's procedure, exclusive of damping effects. The path OABCDEFG represents loading and unloading in side friction. For the point, only compressive loading may take place and the loading and unloading path would be along OABCF.

It is seen that the characteristics of Fig. 2.3(a) are defined essentially by the quantities "Q" and "Ru". "Q" is termed the quake and represents the maximum deformation which may occur elastically. "Ru" is the ultimate static soil resistance, or the load at which a spring K' behaves in a purely plastic manner.

A load-deformation diagram of the sort of Fig. 2.3(a) may be established separately for each spring. Thus

$$K'(m) = \frac{Ru(m)}{Q(m)} \qquad (2)$$

where K'(m) is the spring constant during elastic deformation for external spring m.

Basic Equations—Eqs. 3 through 7 are developed by Smith (3):

$$D(m,t) = D(m,t-1 + 12\Delta t\ V(m,t-1) \qquad (3)$$

$$C(m,t) = D(m,t) - D(m+1,t) \qquad (4)$$

$$F(m,t) = C(m,t)\ K(m) \qquad (5)$$

$$R(m,t) = \left[D(m,t) - D'(m,t) \right] \qquad (6)$$

$$K'(m) \left[1 + J(m)V(m,t-1) \right]$$

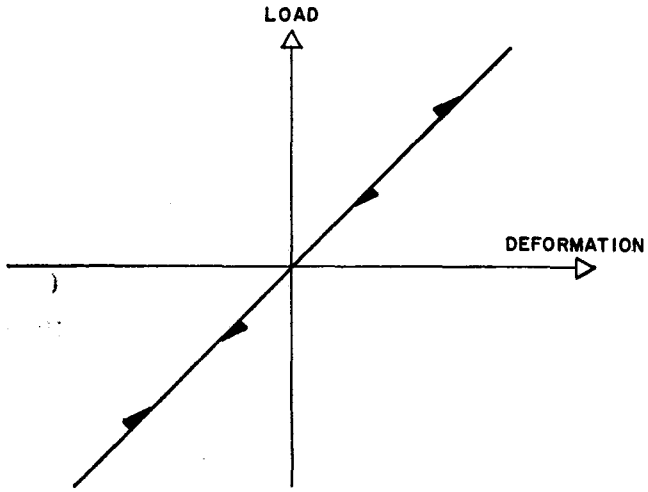

(a) NO INTERNAL DAMPING ASSUMED IN PILE

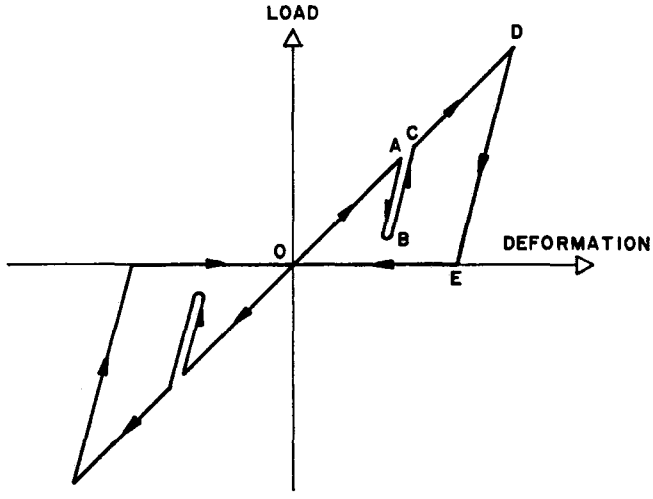

(b) INTERNAL DAMPING

Fig. 2.2. Load-deformation relationships for internal springs.

$$V(m,t) = V(m,t-1) + \left[F(m-1,t) + W(m) - F(m,t) - R(m,t) \right] \frac{g\,\Delta t}{W(m)} \quad (7)$$

where

( ) = functional designation;

m = element number;

t = number of time interval;

Δt = size of time interval (sec);

C(m, t) = compression of internal spring m in time interval t (in.);

D(m, t) = displacement of element m in time interval t (in.);

D'(m, t) = plastic displacement of external spring m in time interval t (in.);

F(m, t) = force in internal spring m in time interval t (lb);

g = acceleration due to gravity (ft per sec^2);

J(m) = damping constant of soil at element m (sec per ft);

K(m) = spring constant associated with internal spring m (lb per in.);

K'(m) = spring constant associated with external spring m (lb per in.);

R(m, t) = force exerted by external spring m on element m in time interval t (lb);

V(m, t) = velocity of element m in time interval t (ft per sec); and

W(m) = weight of element m (lb).

This notation differs slightly from that used by Smith (3). Also, Smith restricts the soil damping constant J to two values, one for the point of the pile in bearing and one for the side of the pile in friction. While the present knowledge of damping behavior of soils perhaps does not justify greater refinement, it is treated in this paper as a function of m for the sake of generality.

The use of a spring constant K(m) implies a load-deformation behavior of the sort shown in Fig. 2.2(a). For this situation, K(m) is the slope of the straight line. Smith develops special relationships to account for internal damping in the capblock and the cushion block. He obtains instead of Eq. 5 the following equation:

$$F(m,t) = \frac{K(m)}{[e(m)]^2} C(m,t) - \left[\frac{1}{[e(m)]^2} - 1 \right] K(m)\, C(m,t)_{max} \quad (8)$$

where

e(m) = coefficient of restitution of internal spring m, and

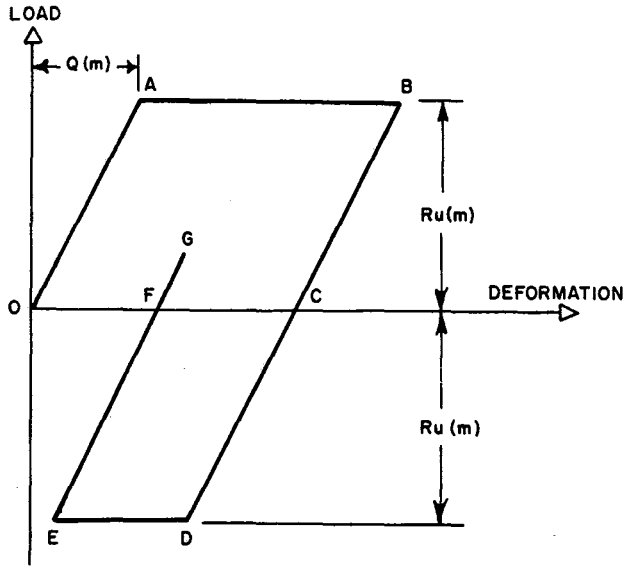

(a) STATIC

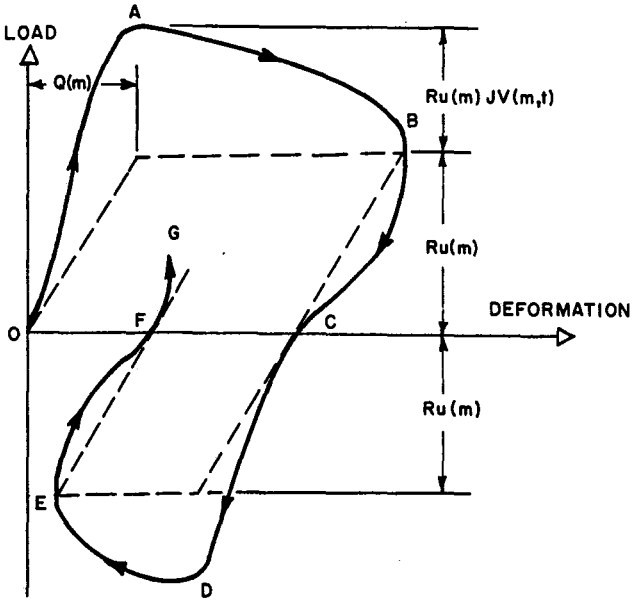

(b) DYNAMIC

Fig. 2.3. Load-deformation characteristics of soil described by Equation 6.

$C(m,t)_{max}$ = temporary maximum value of C(m, t).

With reference to Fig. 2.1, Eq. 8 would be applicable in the calculation of the forces in internal springs m = 1 and m = 2. The load-deformation relationship characterized by Eq. 8 is illustrated by the path OABCDEO in Fig. 2.2(b). For a pile cap or a cushion block no tensile forces can exist; consequently, only this part of the diagram applies. Intermittent unloading-loading is typified by the path ABC, established by control of the quantity $C(m,t)_{max}$ in Eq. 8. The slopes of lines AB,

BC, and DE depend upon the coefficient of restitution e(m).

The Computer Solution

The computations proceed as follows:

1. The initial velocity of the ram is determined from the properties of the pile driver. Other time-dependent quantities are initialized at zero or to produce equilibrium of forces under gravity (see reference 2).

2. Displacements D(m, 1) are calculated by Eq. 3. It is to be noted that V(1, 0) is the initial velocity of the ram.

3. Compressions C(m, 1) are calculated by Eq. 4.

4. Internal spring forces F(m, 1) are calculated by Eq. 5 or Eq. 8, as appropriate.

5. External spring forces R(m, 1) are calculated by Eq. 6.

6. Velocities V(m, 1) are calculated by Eq. 7.

7. The cycle is repeated for successive time intervals.

After many cycles of computation the pile segments reach their maximum downward movement and rebound upward. The permanent set or downward displacement of the pile point D(p) due to the ram blow is equal to OC on Figs. 2.3(a) or 2.3(b).

In Eq. 6 the plastic deformation D'(m, t) for a given external spring follows Fig. 2.3(a) and may be determined by special routines. For example, when D(m, t) is less than Q(m), D'(m, t) is zero; when D(m, t) is greater than Q(m) along line AB (see Fig. 2.3(b), D'(m, t) is equal to D(m, t) — Q(m).

Upon examination it can be seen that Eq. 6 describes a type of Kelvin rheological model as shown in Fig. 2.4. The soil spring K' behaves elastically until the deformation D equals Q and then it yields plastically with a load-deformation property as shown in Fig. 2.3(a). The dashpot J develops a resisting force proportional to the velocity of loading V.

Smith has modified the true Kelvin model as shown by Eq. 6.

This equation will produce a dynamic load-deformation behavior shown by path ABCDEFG in Fig. 2.3(b).

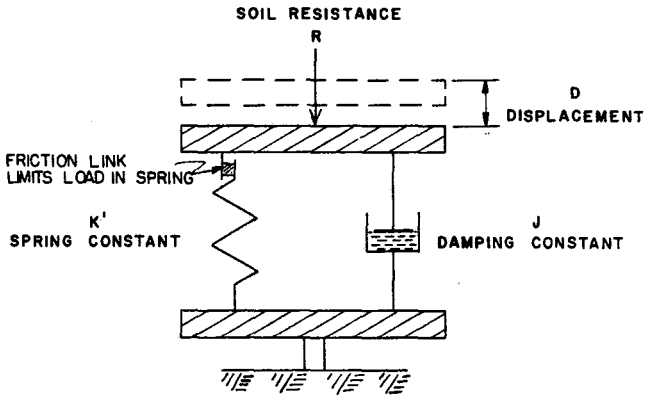

Fig. 2.4. Model used by Smith to describe soil resistance on pile.

If terms in Eq. 6 are examined, it can be seen that Smith's dashpot force is given by

$$[D(m,t) - D'(m,t)]\ K'(m)\ [J(m)\ V(m,t)]$$

The dimensions of J are sec per ft and it is independent of the total soil resistance or size of the pile. The value J is assumed to be constant for a given soil under given conditions as is the static shear strength of the soil from which Ru is determined.

Smith notes that Eq. 6 produces no damping when D(m, t) — D'(m, t) becomes zero. He suggests an alternate equation to be used after D(m, t) first becomes equal to Q(m):

$$R(m,t) = [D(m,t) - D'(m,t)]\ K'(m) + J(m)\ Ru(m)\ V(m,t-1) \qquad (9)$$

Care must be used to satisfy conditions at the point of the pile. Consider Eq. 5. When m = p, where p is the number of the last element of the pile, K(p) is used as the point soil spring and J(p) as the point soil damping constant. Also at the point of the pile, the soil spring must be prevented from exerting tension on the pile point. Therefore, the point soil resistance will follow the path OABC in Fig. 2.3(b). It should be kept in mind that at the pile point the soil is loaded in compression or bearing. The damping constant J(p) in bearing is believed to be larger than the damping constant J(m) in friction along the side of the pile.

Chapter III

SOIL PARAMETERS TO DESCRIBE DYNAMIC SOIL RESISTANCE DURING PILE DRIVING

The soil parameters used to describe the soil resistance in the wave equation are Ru, Q, and J.

Soil Resistance "Ru"

For the side or friction soil resistance Ru is determined by the maximum static soil adhesion or friction against the side of a given pile segment.

$$Ru(m) = fs\ \Sigma_0\ \Delta L \qquad (10)$$

where

fs = max. soil adhesion or friction (lb per ft^2),

Σ_0 = perimeter of pile segment (ft), and

ΔL = length of pile segment (ft).

In cohesionless materials (sands and gravels)

$$fs = \bar{\sigma} \tan \phi' \qquad (11)$$

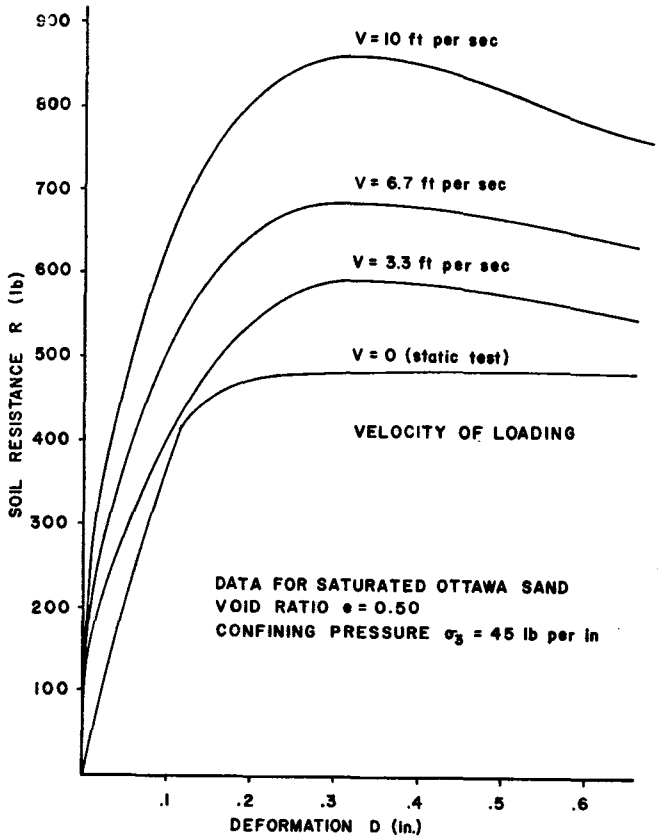

Fig. 3.1. Load-deformation properties of Ottawa sand determined by triaxial tests (specimens nominally 3 in. in diameter by 6.5 in. high).

where

$\overline{\sigma}$ = effective normal stress against the side of the pile (lb per ft^2), and

ϕ' = angle of friction between soil and pile (degrees).

In cohesive soils (clays) fs during driving is the remolded adhesion strength between the soil and pile.

At the point of the pile Ru is determined by the maximum static bearing strength of the soil and is found by

$$Ru = (Qu)\ (Ap) \qquad (12)$$

where

Qu = ultimate bearing capacity of soil (lb per ft^2), and

Ap = area of pile point (ft^2).

In cohesive soils (clays) it is believed that the undisturbed strength of the soil should be used to determine Qu, since the material at the pile point has not yet been remolded.

Quake "Q"

The value of Q, the elastic deformation of the soil is difficult to determine for various types of soils conditions. Various sources of data indicate that values of Q in both friction and point bearing probably range from 0.05 in. to 0.15 in.

Chellis (9) indicates that the most typical value for average pile driving conditions is Q = 0.10 in. If the soil strata immediately underlying the pile tip is very soft, it is possible for Q to go as high as 0.2 in. or more. At the present state of the art and science of pile driving it is recommended that a value of Q = 0.10 in. be used for computer simulation of friction and point soil resistance. However, in particular situations where more precise values of Q are known, they should be used.

Damping Constant "J"

The Texas Transportation Institute has been conducting static and dynamic tests on cohesionless soil samples to determine if Smith's rheological model adequately describes the load-deformation properties of these soils (see Figs. 2.3(a), 2.3(b), and Eq. 6). Triaxial soil tests were conducted on Ottawa sand at different loading velocities. The nominal loading velocities were zero, 3.3, 6.7, and 10 ft per sec and the velocity was essentially constant during any given test. Fig. 3.1 shows typical results from a series of such tests (a detailed description of the tests and procedures has been presented in another report). For illustrative purposes, compare the experimental data in Fig. 3.1 with Fig. 3.2(b) which result from Eq. 6.

From Fig. 3.1, the value of Ru (the maximum static load) is found to be 460 lbs for Ottawa sand with a void ratio of 0.5. The maximum dynamic load during the test at 10 ft per sec is R max = 855 lbs. Since only the maximum static and dynamic soil resistances will be compared, Eq. 6 reduces to (dropping the subscripts):

$$R\ max = Ru\ (1 + JV) \qquad (13)$$

Substituting in the experimental test values

$$855\ lbs = 460\ lbs\ (1 + J \times 10)$$

and solving for J yields

$$J(p) = 0.086$$

If this damping value is used, Eq. 6 appears to do an adequate job of describing the load-deformation behavior of the test specimens in Fig. 3.1.

Fig. 3.2 shows additional data concerning the increase in soil strength as the rate of loading is increased.

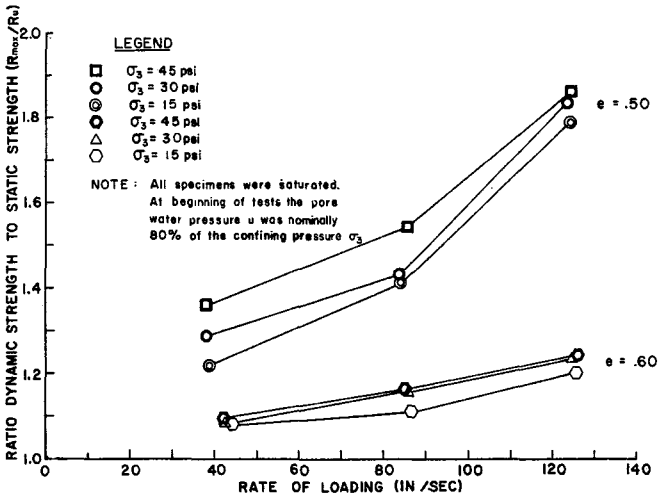

Fig. 3.2. Increase in strength vs rate of loading—Ottawa sand.

Since these tests were confined compression tests it is believed that they simulate to some extent the soil behavior at the pile point. The J value increases as the sand density increases (void ratio e decreases), and it increases as the effective confining stress $\bar{\sigma}_3$ increases.

$$\bar{\sigma}_3 = \sigma_3 - u \qquad (14)$$

where

σ_3 = total confining pressure, and

u = pore water pressure.

For saturated Ottawa sand specimens, J(p) varied from about 0.05 to 0.20. When the sand was dry, J(p) approached zero. These values of J(p) for sand are in agreement with those recommended by Smith (3) and Forehand and Reese (10).

The value of J(p) for cohesive soils (clays) is not presently known. The very limited data available indicate it is at least equal to that for sand. Forehand and Reese believe it ranges from 0.4 to 1.0.

There are no data now available to indicate the value of J(m) in friction along the side of the pile. Smith believes it is smaller than J(p) and recommends J(m) values in friction of about ⅓ those at the point. Research is under way at Texas A&M University which should indicate values of J in friction for different type soils. At the present time J(m) in friction or adhesion will be assumed to be ⅓ of J(p).

Chapter IV

STATIC SOIL RESISTANCE AFTER PILE DRIVING (TIME EFFECT)

Immediately after driving, the total static soil resistance or bearing capacity of the pile would equal the sum of the Ru values discussed in Chapter III. Thus, Ru (total) is the bearing capacity immediately after driving.

$$Ru(\text{total}) = \sum_{m=1}^{m=p} Ru(m) \qquad (15)$$

where

Ru(m) = soil adhesion on friction strength on segments m = 1 to m = p−1 (lb) (Note that this is the strength of the disturbed or remolded soil along the side of the pile), and

Ru(p) = bearing or compressive strength of soil at the pile point m = p (lb). Note this is presently assumed as the strength of the soil in an undisturbed condition.

As time elapses after driving, Ru(m) for m = 1 to p − 1 may increase as the disturbed or remolded soil along the side of the pile reconsolidates and the excess pore water pressure dissipates back to an equilibrium condition. In cohesive soils (clays) the increase in strength upon reconsolidation (sometimes referred to as "set-up") is often considerable.

The bearing capacity of the pile will increase as the remolded or disturbed clay along the side of the pile reconsolidates and gains strength, since the adhesion or friction strength of clay is generally restored with the passage of time. Loading tests at increasing intervals of time show that ultimate adhesion is approximately equal to the undisturbed cohesion. Therefore, the amount of increase in bearing capacity with time is related to the sensitivity of the clay* and the load carrying capacity provided by friction.

Fig. 4.1 illustrates the time effect or "set-up" of a pile driven in a cohesive soil. In cohesionless soils (sands and gravels) the friction strength of the soil will usually change very little. Normally, the value of Ru(p) at the pile point changes very little since it is essentially undisturbed.

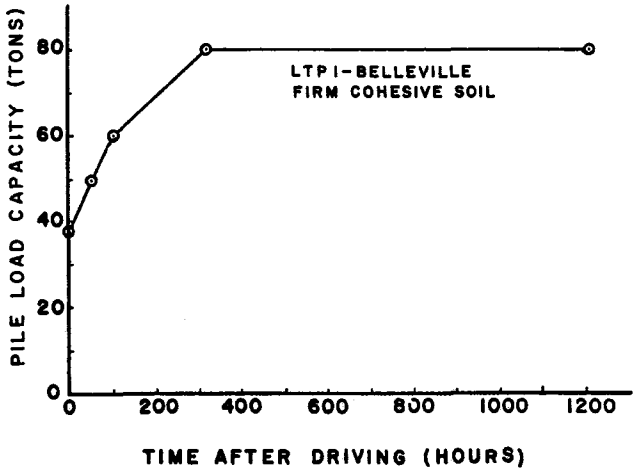

Fig. 4.1. "Set-up" or recovery of strength after driving in cohesive soil (after Reference 14).

*Sensitivity of clay = $\frac{\text{undisturbed strength}}{\text{remolded strength}}$.

Chapter V

USE OF THE WAVE EQUATION TO PREDICT PILE LOAD BEARING CAPACITY

The previous chapters have shown how the hammer pile-soil system can be simulated and analyzed by the wave equation to determine the dynamic behavior of piling during driving. *With this simulation the driving stresses and penetration of the pile can be computed* using the given conditions such as driving equipment and soil resistance.

The converse of this problem is to use this method of analysis to determine soil resistance during driving. In the field the pile penetration or permanent set per blow is observed and this can be translated into the soil resistance if all other variables are known.

For example:

PILE: 72 ft steel step taper pile

HAMMER: No. 00 Raymond
Efficiency = 80%
Ram Weight = 10,000 lb
Energy = 32,500 ft lb

CAPBLOCK: Micarta
K = 6,600,000 lb per in
e = 0.8

ASSUMED SOIL PARAMETERS:
J(p) point = 0.15 sec per ft
J(m) side = 0.05 sec per ft
Q(p) point = 0.10 in.
Q(m) side = 0.10 in.

Soil is a soft marine deposit of fine sand, silt, and muck, with the pile point founded on a dense layer of sand and gravel.

Referring to Fig. 5.1 we have two assumed soil distributions:

Curve I: 25% side friction (triangular distribution)
75% point bearing.

Curve II: 10% side friction (triangular distribution)
90% point bearing.

This information is used to simulate the system to be analyzed by the wave equation. A total soil resistance Ru(total) is assumed by the computer and the wave equation program then computes the pile penetration or "permanent set" when driven against this Ru(total). The reciprocal of "permanent set" is usually computed to convert this to blows per in.

The computer then selects a higher Ru(total) and computes the corresponding blows per in. This is done several times until enough points are generated to develop a curve relating blows per in. to Ru(total) as shown in Fig. 5.1 (two curves for two different distributions of soil resistance are shown).

In the field if driving had ceased when t
ance to penetration was 10 blows per in. (a p
set equal to 0.1 in. per blow), then the ultimate pile load bearing capacity immediately after driving should have been approximately 370 to 380 tons as shown on Fig. 5.1. It is again emphasized that this Ru(total) is the total *static* soil resistance encountered during driving, since the increased dynamic resistance was considered in the analysis by use of J. If the soil resistance is predominantly due to cohesionless materials such as sands and gravels, the time effect or soil "set-up" tending to increase the pile bearing capacity will be small or negligible. On the other hand, if the soil is a cohesive clay, the time effect or soil "set-up" might increase the bearing capacity as discussed in Chapter IV. The magnitude of this "set-up" can be estimated if the "sensitivity" of the clay is known. It can also be conservatively disregarded since the "set-up" bearing capacity should in most cases be greater than that predicted by a graph similar to Fig. 5.1.

In developing the curves of Fig. 5.1, it was necessary to assume the following soil parameters:

1. Distribution of soil resistance.

PILE: 72 ft. Step Taper, 12 ft. steps, No. 1 to No. 6
HAMMER: No. 00 Raymond
SHELL: Step Taper Corrugated
CAPBLOCK: Micarta; Coeff. of Rest. = .80;
K = 6,600,000 ppi
DISTRIBUTION OF RESISTANCE:
Curve I: 25% Side (Triangular Distribution);
75% Point
Curve II: 10% Side (Triangular Distribution);
90% Point
CONSTANTS:
J (Point) = 0.15; J (Side) = 0.05
Q (Point) = 0.10; Q (Side) = 0.10

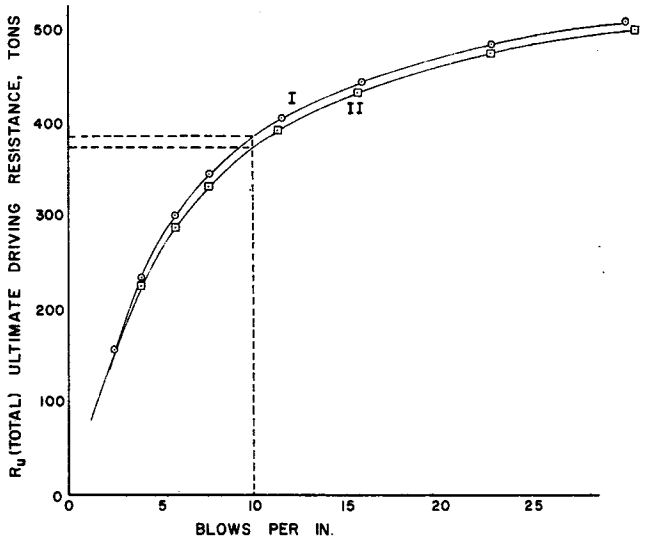

Fig. 5.1. Ultimate driving resistance vs blows per inch for an example problem.

2. Soil Quake "Q."
3. Soil damping constant "J."

Small variations in the distribution of soil resistance between side friction and point bearing will not affect the wave equation results significantly as illustrated by Curves I and II on Fig. 5.1. Also, it is usually known whether the pile bearing capacity is essentially all point bearing, all friction, 50% point bearing and 50% friction, etc. All that is required is a reasonable estimate of the situation.

For most conditions an assumption of soil quake Q = 0.1 in. is satisfactory (see Chapter III).

The significance of the soil damping values on pile driving analysis will be discussed later in this paper. The value of J(m) is assumed to be ⅓ of J(p).

Chapter VI

SUMMARY OF PROBLEM INFORMATION

In order to predict the probable soil damping values for various soils, a number of cases had to be solved to develop a series of curves similar to those of Fig. 5.1.

The pile-driving problems studied herein were for piles driven and tested in three general locations—along the Texas Gulf Coast, Arkansas River, and in the state of Michigan. Nine different hammers were used to drive prestressed concrete, steel H, flute-taper, and pipe piles ranging from 30 to 180 ft long, under a variety of driving conditions. More detailed information is listed in the following tables.

Table 6.1 lists the hammer properties and operating characteristics for each case. Tables 6.2 and 6.3 list the properties of the piles and the driving accessories used. Additional information regarding the Arkansas cases can be found in reference (14), and for the Michigan cases in reference (11).

The Texas Gulf Coast studies were performed by the authors as a part of the present research and are therefore fully reported herein.

TABLE 6.1. HAMMER PROPERTIES AND OPERATING CHARACTERISTICS

Location	Load Test Pile	Hammer Manufacturer	Hammer Type	Ram Weight (lb)	Anvil Weight (lb)	Rated Energy (ft-lb)	Hammer Efficiency (%)	Ram Velocity at Impact (ft/sec)	Explosive Force (lb)
Victoria	35	Vulcan	#1 -	5000	none	15000	60	10.8	
	40	Vulcan	#1 -	5000	none	15000	60	10.8	
	45	Vulcan	#1 -	5000	none	15000	60	10.8	
Chocolate Bayou	40	Link Belt	520 -	5070	1179	30000		16.3	98000
	60	Link Belt	520 -	5070	1179	30000		16.3	98000
Houston	30	Delmag	D-22	4850	1147	39700		19.9	93700
Copano Bay	58	Vulcan	014 -	14000	none	42000	90	13.2	
	103	Vulcan	014 -	14000	none	42000	90	13.2	
Arkansas	1	Vulcan	140 C	14000	none	36000	78	11.6	
	2	Vulcan	140 C	14000	none	36000	78	11.6	
	3	Vulcan	140 C	14000	none	36000	78	11.6	
	4	Vulcan	140 C	14000	none	36000	78	11.6	
	5	Vulcan	140 C	14000	none	36000	78	11.6	
	6	Vulcan	80 C	8000	none	24450	84	12.8	
	7	Vulcan	80 C	8000	none	24450	84	12.8	
	16	Vulcan	140 C	14000	none	36000	78	11.6	
Belleville	1	Vulcan	#1 -	5000		15000	60	10.80	
	3	MKT	DE-30	2800	774	22400		17.94	98000
	4	Link Belt	312 -	3855	1188	18000		15.84	98000
	5	Delmag	D-12	2750	754	22600		21.00	93700
	6	Vulcan	#1 -	5000		15000	60	10.80	
Detroit	1	Vulcan	#1 -	5000		15000	60	10.80	
	2	Vulcan	#1 -	5000		15000	60	10.80	
	7	MKT	DE-30	2800	774	22400		17.94	98000
	8	Vulcan	#1 -	5000		15000	60	10.80	
	10	Link Belt	312 -	3855	1188	18000		15.84	98000
Muskegon	2	Vulcan	#1 -	5000		15000	60	10.80	
	3	Vulcan	#1 -	5000		15000	60	10.80	
	4	Vulcan	#1 -	5000		15000	60	10.80	
	6	Delmag	D-22	4850	1147	39700		17.26	158700
	7	Vulcan	80-C	8000		24450	83.3	12.80	
	8	Delmag	D-22	4850	1147	39700		17.26	158700
	9	Vulcan	80-C	8000		24450	83.3	12.80	

TABLE 6.2. PROPERTIES OF PILES AND DRIVING ACCESSORIES

Location	Load Test Pile	Pile Type	Pile Length (ft)	Helmet Weight (lb)	Type Capblock	Type Cushion Block	e** of Capblock	e** of Cushion Block
Victoria	35	16″ sq. P.C.	35	1000	(a)	6″ Plywood fir	0.5	0.5
	40	16″ sq. P.C.	40	1000	(a)	6″ Plywood fir	0.5	0.5
	45	16″ sq. P.C.	45	1000	(a)	6″ Plywood fir	0.5	0.5
Chocolate Bayou	40	16″ sq. P.C.	40	1300	(b)	6″ Plywood fir	0.8	0.5
	60	16″ sq. P.C.	60	1300	(b)	6″ Plywood fir	0.8	0.5
Houston	30	*	30	1460	(c)	6″ Plywood fir	0.8	0.5
Copano Bay	58	18″ sq. P.C.	58	3000	(d)	6″ Gum or Oak	0.5	0.5
	103	18″ sq. P.C.	103	3000	(d)	6″ Gum or Oak	0.5	0.5
Arkansas	1	12″ Pipe	55	1710		none	0.8	
	2	16″ Pipe	55	1710		none	0.8	
	3	20″ Pipe	55	1710		none	0.8	
	4	16″ Pipe	45	1710		none	0.8	
	5	16″ sq. P.C.	55	1710			0.8	0.3
	6	14BP73	42	1220		none	0.8	
	7	14BP73	55	1220		none	0.8	
	16	16″ Pipe	55	1220		none	0.8	
Belleville	1	12″ Dia. 25″ wall	45.5	1000	(e)	none	0.5	
	3	(1)	62.0	1000	(f)	none	0.5	
	4	12″ Dia. 25″ wall	67.6	1381	(g)	none	0.5	
	5	12″ Dia. 179″ wall	67.8	1000	(h)	none	0.5	
	6	12x12 H-pile	59.1	1000	(e)	none	0.5	
Detroit	1	12″ Dia. #7 gage	71.9	1000	(e)	none	0.5	
	2	12″ Dia. #7 gage	80.7	1000	(e)	none	0.5	
	7	12″ Dia. #7 gage	83.2	1400	(c)	none	0.5	
	8	12x12 H-pile	83.3	1000	(e)	none	0.5	
	10	12″ Dia. 23″ wall	83.1	1381	(g)	none	0.5	
Muskegon	2	12″ Dia. 23″ wall	60.0	1000	(e)	none	0.5	
	3	12″ Dia. #7 gage	60.2	1000	(e)	none	0.5	
	4	12″ Dia. 23″ wall	60.0	1000	(e)	none	0.5	
	6	12″ Dia. 25″ wall	130	1463	(h)	none	0.5	
	7	12″ Dia. 25″ wall	180.4	2140	(i)	none	0.5	
	8	12″ Dia. 25″ wall	180.1	1463	(h)	none	0.5	
	9	12″ Dia. 25″ wall	130.2	2140	(i)	none	0.5	

*14″ square prestressed concrete, tapered from 14″ to 8″ at tip of pile.

**e = coefficient of restitution.

(a) Garlock asbestos disk, 11¼ in. diameter by 3 in. thick with 2 steel plates 11¼ in. by ¾ in. thick.
(b) Alternating layers of phenol fiber plates, 11 in. diameter by ½ in. thick with 4 aluminum plates 11 in. diameter by ⅛ in. thick.
(c) Plywood fir, ¾ in. thick.
(d) Gum, ¾ in. thick.
(e) Oak block, 11¼ in. diameter by 6¼ in. thick on top of two steel plates each 11¼ in. diameter by ¾ in. thick.
(f) Oak block, 18½ in. diameter by 2¼ in. thick (grain vertical).
(g) Alternating layers of 5 micarta fiber plates 11 in. diameter by ½ in. thick.
(h) German oak block, 15 in. x 15 in. x 5 in. thick under steel block, 15 in. x 15 in. x 3 in. thick.
(i) Two micarta fiber blocks each 14 in. diameter by 5 in. thick.

TABLE 6.3. PHYSICAL PROPERTIES OF CONCRETE IN LOAD TEST PILES

Concrete Property	LOCATION AND LOAD TEST PILE			
	Victoria 35, 40, and 45	Chocolate Bayou 40 and 60	Houston 30	Copano Bay 58 and 103
Unit Weight (pcf)	152	155	152	149
Compressive Strength 6 in. x 12 in. Cyl. (psi)	6342	6780	6607	6490
Flexural Strength 3 in. x 4 in. x 16 in. Prism (psi)	1133	1000		1000
Modulus of Elasticity Static (psi)	7.64×10^6	7.75×10^6	7.61×10	6.61×10^6
Modulus of Elasticity Dynamic (psi)	7.80×10^6	7.65×10^6	7.31×10^6	7.73×10^6
Poisson's Ratio Dynamic (psi)	0.20	0.28		0.20
Tensile Strength Split cylinder (psi)		600	639	

Chapter VII

DETERMINATION OF SOIL RESISTANCE DISTRIBUTION

In order to obtain the best correlation between theoretical and experimental results, the actual distribution of the soil resistance acting on the pile was determined. This distribution was found by placing strain gages along the pile before driving, and recording the loads at each gage point during the load test. The soil legend used throughout the report (unless otherwise noted) is shown in Fig. B.1 in Appendix B.

TABLE 7.1. PERCENT OF TOTAL SOIL RESISTANCE CARRIED BY EACH TYPE OF SOIL = ΔR_i

Location	Load Test Pile	Side Resistance			Point Resistance
		ΔR_{clay} = % RUT Clay / 100	ΔR_{sand} = % RUT Sand / 100	ΔR_{silt} % RUT Silt / 100	$\Delta R_{(type)}$ % RUT (type) / 100
Victoria	35	0.30	0.15	0.00	0.55 (sand)
	40	0.29	0.27	0.00	0.44 (sand)
	45	0.31	0.03	0.03	0.65 (sand & silt)
Chocolate Bayou	40	0.42	0.19	0.23	0.16 (sand)
	60	0.40	0.20	0.20	0.20 (sand & silt)
Houston	30	0.20	0.08	0.10	0.62 (silt & clay)
Copano Bay	58	0.64	0.08	0.08	0.20 (clay)
	103	0.00	0.20	0.20	0.60 (sand & silt)
Arkansas	1	0.00	0.76	0.00	0.24 (sand)
	2	0.00	0.70	0.00	0.30 (sand)
	3	0.00	0.66	0.00	0.34 (sand)
	4	0.00	0.42	0.00	0.58 (sand)
	5	0.00	0.42	0.00	0.58 (sand)
	6	0.00	0.22	0.00	0.78 (sand)
	7	0.00	0.22	0.00	0.78 (sand)
	16	0.00	0.71	0.00	0.29 (sand)
Belleville	1	0.94			0.06 (clay)
	3	0.34	0.08	0.08	0.50 (sand & silt)
	4	0.20	0.05	0.05	0.70 (clay)
	5	0.20	0.05	0.05	0.70 (clay)
	6	0.64	0.08	0.08	0.20 (sand & silt)
Detroit	1	0.64			0.36 (clay)
	2	0.15			0.85 (clay)
	7	0.35			0.65 (clay)
	8	0.34			0.66 (clay)
	10	0.19			0.81 (clay)
Muskegon	2		0.85		0.15 (sand)
	3		0.92		0.08 (sand)
	4		0.95		0.05 (sand)
	6		0.75		0.25 (sand)
	7	0.30	0.30		0.40 (sand)
	8	0.30	0.30		0.40 (sand)
	9		0.75		0.25 (sand)

Knowing the load in the pile at any given point, the load which had been transferred to the soil above that point can be found, thus determining the load-transfer curves of Figs. B.1 thru B.22 in Appendix B. These figures also present the type of soil encountered at each location. In the Copano Bay cases only the soil data are presented since no load-transfer data were obtained (see Fig. B.8 in Appendix B).

In most of the Texas Gulf Coast studies and the Arkansas cases, load-transfer curves were available to determine how much resistance was transferred to each soil strata. When these data were not available, the resistance distribution was determined from soil tests. The soil profiles and load capacities for the cases in which load-transfer curves were not known are also presented in Appendix B. A summary of the total load carried by each type of soil is given in Table 7.1.

Computer Idealization

Using the load-transfer curves or the soil test data presented in Appendix B, the soil distributions to be used in the wave equation were determined. These distributions are illustrated in Figs. B.9 thru B.22.

Although Smith's idealization was discussed in Chapter II, the idealized Texas Gulf Coast piles are shown in Figs. B.9 through B.16 to further illustrate this method of analysis.

Note that in the case of the steam hammers, K(1) is taken as the spring rate of the cushion, where as for the diesel hammers, the spring rate of the ram itself must be interposed between the ram and anvil. Recommended solutions to the problems arising when "steel-on-steel" impact occurs in the system (as for the diesel hammer case) have been noted (4), (8), and will therefore not be discussed at this time.

Chapter VIII

DETERMINATION OF MAXIMUM SOIL RESISTANCES

Several different field methods were used to determine load settlement curves of the piles tested, and also the method of interpreting these curves varied. This made the choice of a load capacity for any given pile more difficult.

For example, the Texas Gulf Coast piles were load tested by one or more of the following methods:

1. a quick load test method wherein the test load was applied in 5- to 15-ton increments at 2½ minute intervals,

2. the AASHO 48-24 hour test, and/or

3. a slow test in which 5- to 15-ton increments of load were applied 2 hours after all measurable settlement due to the previous loading had ceased.

Further, the Michigan piles were first "cycled" to failure before final testing, thereby increasing their measured load capacity (12), whereas the Texas piles were rated on the first load cycle.

The data obtained for the Texas Gulf Coast load test piles are included in Appendix C.

Different methods of interpreting the load-settlement data were also used, including the following: net settlement, gross settlement, method of tangents and maximum rate of settlement. However, each report did establish a value predicted by the method of tangents, and therefore this method was used for correlation with the wave equation.

The use of the method of tangents in determining the maximum static resistance is illustrated in Fig. 8.1. One line originates at zero load and is drawn tangent to the elastic portion of the gross settlement curve, while the second line is tangent through two or more points of the curve at the maximum load. The resulting soil resistances are summarized in Table 8.1.

It must be emphasized that these are not the resistances which were acting on the piles during driving. As noted in Table 8.1, the driving and load testing dates

TABLE 8.1. DRIVING AND TEST LOADING INFORMATION

Location	Load Test Pile	Pile Embedment (ft)	Average Blows per Inch Over Last Foot (blows/in.)	Time Between Driving and Load Test (days)	R_{LT} (Ultimate Test Load) (tons)
Victoria	35	26.6	5.2	8	104
	40	33.2	4.3	34	80
	45	29.5	32.9	45	176
Chocolate Bayou	40	36.0	2.0	19	105
	60	56.5	42.0	14	Over 200
Houston	30	26.5	3.2	14	170
Copano Bay	58	44.4	2.2	46	Over 200
	103	83.5	2.4	78	150
Arkansas	1	53.1	1.3		140
	2	52.8	3.2		190
	3	53.0	3.7		215
	4	40.2	3.5		170
	5	51.0	4.0		250
	6	40.0	1.3		140
	7	52.1	2.6		200
	16	52.7	2.0		140
Belleville	1	44.4	11.0	51	80
	3	50.9	58.0	50	171
	4	56.5	60.0	50	345
	5	56.7	34.0	57	346
	6	58.0	49.0	51	206
Detroit	1	69.5	2.0	12	28
	2	78.6	36.0	8	165
	7	81.1	30.0	22	159
	8	81.1	37.0	14	180
	10	81.0	20.0	23	225
Muskegon	2	58.0	8.0	26	100
	3	57.8	4.0	26	55
	4	58.0	2.1	23	42
	6	128.0	3.0	18	273
	7	178.4	42.6	25	Over 370
	8	178.2	64.0	19	Over 370
	9	128.2	5.5	25	235

were widely separated, thereby allowing the soil to consolidate or "set up."

A determination of how much this resistance will change between driving and testing is always difficult. The Michigan report does present the results of two piles load tested immediately after driving and 12 to 50 days later from which a "set-up" factor of 2.0 was noted in firm and stiff clays (13). While extrapolation of such data to other areas is always risky, the lack of information for the other sites prompted the use of the 2.0 "set-up" factor for clays, and no "set-up" for other soils ("set-up" factor equal 1.0).

Knowing the resistance distributions listed in Table 7.1, and the soil "set-up" factors, it is possible to transform the load test results given in Table 8.1 into the static soil resistances which were acting on the piles at the time of driving. For example, if a pile which was driven into a firm clay and load tested 51 days after driving gave an indicated soil resistance of 160 kips, it would probably have indicated a value of 160/2 = 80 kips if it had been load tested immediately after driving. Similarly, the indicated soil resistance of a pile driven in sand should be the same immediately after driving as later since no set-up is involved.

When the pile is acted on by a combination of soils having different set-up factors the following general equation can be used to transform the "after set-up" resistance into the static resistance immediately after driving by:

$$R_{dr} = (R_{LT})\ (k) \qquad (16)$$

where

$$k = \left[1.0 - \sum \left(\frac{\Delta R_i}{R_{LT}} \right) \left(\frac{F_i - 1.0}{F_i} \right) \right] \qquad (17)$$

R_{LT} = total soil resistance determined by load test after all set-up had ceased,

ΔR_i = the ratio of the amount of resistance of each type of soil "i," to the total soil resistance, both determined after set-up has ceased, and listed in Table 7.1, and

F_i = the set-up factor corresponding to the soil type "i."

As an example of Eq. 16, assume that a pile, driven several months ago was recently load tested with the following results:

1. Total resistance = 2200 kip.
2. Resistance due to soft clay (set-up = 3) = 900 kip.

TABLE 8.2. DETERMINATION OF STATIC SOIL RESISTANCE AT TIME OF DRIVING FROM LOAD TEST RESULTS

Location	Load Test Pile	Ratio of Total Soil Resistance with Fs = 2 / 100.0	Ratio Total Soil Resistance with Fs = 1 / 100.0	k	R_{LT} (kips)	R_{dr} (kips)
Victoria	35	0.30	0.70	0.85	208	176
	40	0.30	0.70	0.85	160	136
	45	0.30	0.70	0.85	352	300
Chocolate Bayou	40	0.42	0.58	0.79	210	166
	60	0.40	0.60	0.80	Over 400	Over 320
Houston	30	0.51	0.49	0.75	340	255
Copano Bay	58	0.84	0.16	0.58	Over 400	Over 230
	103	0.00	1.00	1.00	300	300
Arkansas	1	0.00	1.00	1.00	280	280
	2	0.00	1.00	1.00	380	380
	3	0.00	1.00	1.00	430	340
	4	0.00	1.00	1.00	340	343
	5	0.00	1.00	1.00	500	500
	6	0.00	1.00	1.00	280	280
	7	0.00	1.00	1.00	400	400
	16	0.00	1.00	1.00	280	280
Belleville	1	1.00	0.00		160	80
	3	0.34	0.66	0.83	342	284
	4	0.90	0.10	0.55	690	379
	5	0.90	0.10	0.55	692	381
	6	0.64	0.36	0.68	412	280
Detroit	1	1.00	0.00	0.50	56	28
	2	1.00	0.00	0.50	330	165
	7	1.00	0.00	0.50	318	159
	8	1.00	0.00	0.50	360	180
	10	1.00	0.00	0.50	450	225
Muskegon	2	0.00	1.00	1.00	200	200
	3	0.00	1.00	1.00	110	110
	4	0.00	1.00	1.00	85	85
	6	0.00	1.00	1.00	540	540
	7	0.30	0.70	0.85	Over 740	Over 680
	8	0.30	0.70	0.85	Over 740	Over 680
	9	0.00	1.00	1.00	470	470

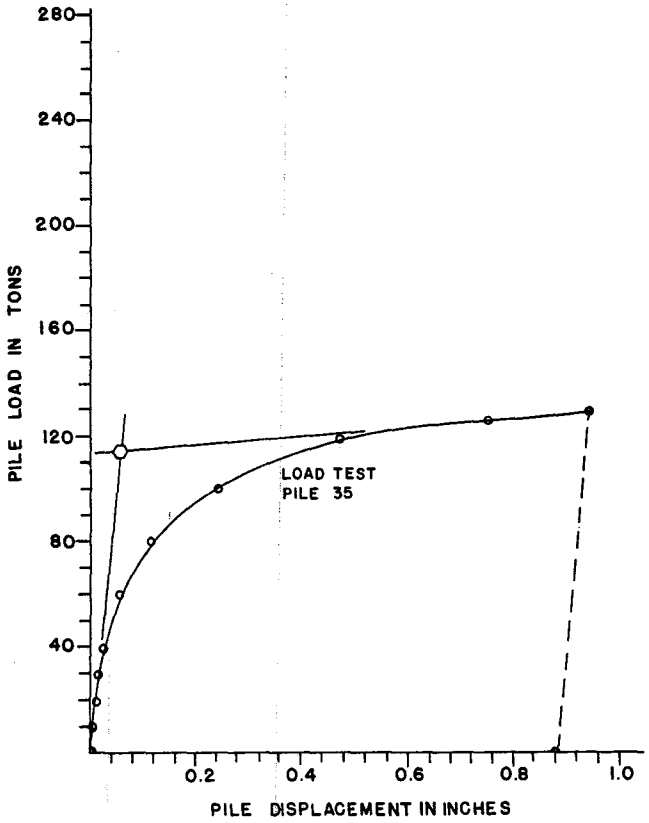

Fig. 8.1. Pile load tests for Victoria Bridge Pile 35.

3. Resistance due to firm clay (set-up = 2) = 800 kip.

4. Resistance due to sand (set-up = 1) = 500 kip.

Then by Eq. 16, the resistance which would have been measured immediately after driving is:

$$R_{dr} = 2200\left[1.0 - \left(\frac{900}{2200}\right)\left(\frac{3-1}{3}\right) - \left(\frac{800}{2200}\right)\left(\frac{2-1}{2}\right) - \left(\frac{500}{2200}\right)\left(\frac{1-1}{1}\right)\right]$$

$$= 2200\ [1.0 - 0.273 - 0.182 - 0]$$

$$= 2200\ [0.545]$$

$$R_{dr} = 1200 \text{ kips}$$

This can be checked by noting that each soil's portion of R_{dr} times its set-up factor gives the original value of R_{LT}:

3 (R_{dr} of soft clay) = 3 (300 kips) = 900 kips
2 (R_{dr} of firm clay) = 2 (400 kips) = 800 kips
1 (R_{dr} of sand) = 1 (500 kips) = 500 kips

R_{LT} Total = 2200 kips

Table 8.2 lists the soil resistance immediately after driving found for each case. These values will be used to solve for the soil damping constants for various soils and to check the probable accuracy of the values determined.

Chapter IX

DETERMINATION OF SOIL DAMPING CONSTANTS

As previously mentioned, the determination of soil damping values for various soils required a number of curves similar to those of Fig. 5.1. For this purpose the Texas, Arkansas, and Michigan cases were solved using varying soil damping constants as shown in Fig. 9.1. The other results are presented in Figs. D.2 through D.33 in Appendix D. These figures show the effect of various soil damping constants on RU(total) soil resistance at time of driving compared to the pile penetration shown as blows per inch. In each case, J(m) was taken as ⅓ J(p). The load test result and the indicated soil resistance immediately after driving (both determined in Chapter VIII) are also given in each case.

Actually the cases solved were extremely well suited to determining the soil damping constants involved for the following reasons:

1. All of the Arkansas piles and several of the other piles were driven in sand only. Thus these cases could be used to evaluate the damping constant for sand without involving the damping constants of other soils.

2. A sufficient number of piles were also driven only in clays, enabling the solution for soil damping of clay independent of that for sand.

3. There remained a large number of piles which were driven in mixtures of both clays and sands, from which a method to determine the combined soil damping constants could be found.

Determining the Soil Damping Constants for Sand and Clay

Although several methods for determining damping constants for each type of soil were tried, the most accurate results were finally obtained by trial and error.

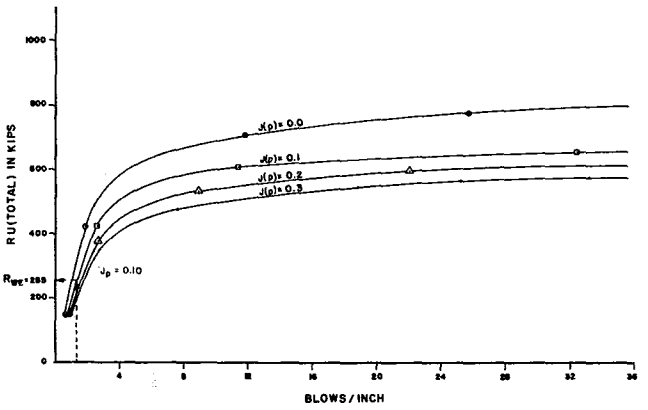

Fig. 9.1. Blows/inch vs RU (total) for Arkansas Load Test Pile 1.

TABLE 9.1. ERRORS CAUSED BY ASSUMING J(p) = 0.1 FOR SAND
(For Sand-Supported Piles Only)

Location	Load Test Pile	R_{dr} (Resistance at Time of Driving) (kips)	R_{WE} (Indicated Soil Resistance) (kips)	% Error in R_{dr} $\left(\frac{R_{WE} - R_{dr}}{R_{dr}}\right)(100)$
Arkansas	1	280	255	− 9
	2	380	495	+30
	3	430	530	+23
	4	340	370	+ 9
	5	500	380	−24
	6	280	170	−39
	7	400	310	−23
	16	280	380	+36
Copano Bay	103	300	320	+ 7
Muskegon	2	200	195	− 3
	3	110	145	+32
	4	85	110	+29
	6	540	310	−43
	9	470	270	−43
			Total	−18
			Mean or Average % Error	≃ − 1

For example, the value for sand found from Arkansas Load Test Pile No. 1 (see Fig. 9.1) is 0.05. When this value, along with those obtained for the other sand-supported piles are averaged, a mean value of J(p) = 0.14 is found.

Substituting this value back into Fig. 9.1 yields an indicated soil resistance of 230 kips rather than the correct value of 280 kips, an error or (280 − 230)/280 = 18%. Further, when all the predicted resistances of sand-supported piles are averaged, the average error using J(p) = 0.14 is much greater than if J(p) = 0.10 is used.

Thus, the soil damping constants determined herein are actually those which best fit the data. As noted in Tables 9.1 and 9.2, the most accurate soil damping constants (i.e., the values which result in the least deviation between actual and predicted soil resistance) were found to be 0.1 for sand and 0.3 for clay. The percent error for each case due to these assumed values are listed in Tables 9.1 and 9.2.

Determination of Soil Damping Constants for Piles Supported by Both Sand and Clay

Since more than one soil, and therefore more than a single damping constant is involved, it seems reasonable (for a first trial at least) to proportion J(m) and J(p) relative to the type of soil supporting the pile by the equation

$$J(p) = \Sigma \Delta R_i \times J(p)_i \qquad (18)$$

where ΔR_i has been defined (see Eq. 17) and $J(p)_i$ is the soil damping constant for soil i (0.1 for sand, 0.3 for clay).

Thus if the pile is supported by only sand, J = 0.1.

TABLE 9.2. ERROR CAUSED BY ASSUMING J(p) = 0.3 FOR CLAY
(For Clay-Supported Piles Only)

Location	Load Test Pile	R_{dr}*** (Resistance at Time of Driving) (kips)	R_{WE} (Indicated Soil Resistance) (kips)	% Error in R_{dr} $\left(\frac{R_{WE} - R_{dr}}{R_{dr}}\right)(100)$ A	B
Belleville	1**	80	200	+150	omit
	4*	379	305	− 17	−17
	5*	381	260	− 30	−30
Detroit	1**	28	70	+130	omit
	2	165	155	− 6	− 6
	7	159	205	+ 29	+29
	8	180	240	+ 33	+33
	10	225	250	+ 11	+11
				Total A = +300	Total B = +20

Average % Error (A) = 300/8 = +38
(B) = 20/6 = +3.33

*90% clay-supported piles.
**The values for these piles were questionable.
***R_{dr} for piles driven in clay were corrected actual load test measurements to account for soil "set-up" (See Table 8.2).

TABLE 9.3. ERROR CAUSED BY ASSUMING A COMBINED J(p) = 0.1 FOR SAND AND J(p) = 0.3 FOR CLAY USING EQ. 18 (For Piles Supported by Both Sand and Clay)

Location	Load Test Pile	$\Delta R_{clay} \times 0.3$	$\Delta R_{sand} \times 0.1$	J(p) (sec/ft)	R_{dr}** (Resistance at Time of Driving) (kips)	R_{WE} (Indicated Soil Resistance) (kips)	% Error in R_{dr} $\left(\frac{R_{WE} - R_{dr}}{R_{dr}}\right)$ (100)
Victoria	35	.090	.070	0.16	176	170	− 3
	40	.087	.071	0.16	136	148	+ 9
	45	.093	.069	0.16	300	380	+27
Chocolate Bayou	40	.126	.058	0.18	166	150	−10
	60	.120	.060	0.18	*	740	
Houston	30	.153	.049	0.20	255	290	+14
Copano Bay	58	.252	.016	0.27	*	260	
Belleville	3	.102	.066	0.17	284	265	− 7
	4	.270	.010	0.28	379	305	−20
	5	.270	.010	0.28	381	260	−32
	6	.192	.036	0.23	280	305	+ 9
Muskegon	7	.090	.070	0.16	*	320	
	8	.090	.070	0.16	*	295	
						Total =	−13
					Average % Error = $\frac{-13}{9}$ =		−1.45

*Indicates piles which exceeded the testing equipment's capacity, and could not be load-tested to failure.
**R_{dr} for these piles are corrected actual load test measurements to account for soil "set-up" (See Table 8.2).

If half of the resistance is provided by sand and ½ by clay, J(p) = (½) (0.1) + (½) (0.3) = 0.2, while if the pile is supported only by clay, J(p) = 0.3. Actually, this method appears quite accurate.

To illustrate the method, the damping constant for Victoria Load Test Pile 35 will be determined (see Fig. D.1 in Appendix D). As noted in Table 7.1, this pile is supported by 70% sand and 30% clay. Thus, J(p) = (0.7) (0.1) + (0.3) (0.3) = 0.16. If this value is substituted into Fig. D.1, the resistance R_{WE} = 170 kips is indicated by the wave equation, whereas the actual resistance to penetration at the time of driving, R_{dr}, was 176 kips.

The results of applying this method to each of the piles supported by both sand and clay are listed in Table 9.3.

Chapter X

COMPARISON OF WAVE EQUATION PREDICTIONS WITH FIELD TESTS

Correlation of wave equation solutions with full-scale load tests to failure have provided a degree of confidence in this method of predicting the soil resistance on a pile at the time of driving. Comparisons are made with 31 full-scale load tests.

Fig. 10.1 compares the wave equation predictions (R_{WE}) with the soil resistance at the time of driving (R_{dr}) as determined by load tests on piles driven in "SANDS." Data plotted in this figure were obtained from Table 9.1. The average accuracy of the wave equation prediction was approximately ±25% for piles supported in sand.

Fig. 10.2 compares the wave equation prediction (R_{WE}) with the soil resistance at the time of driving (R_{dr}) as estimated from load test results on piles driven in "CLAYS." Data presented in this figure were obtained from Table 9.2. The average accuracy for these piles driven in clays was approximately ±40%.

Fig. 10.3 compares the wave equation prediction

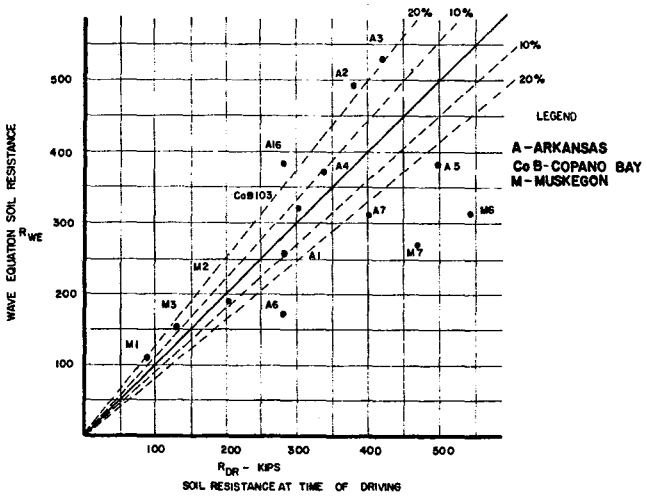

Fig. 10.1. Comparison of wave equation soil resistance to soil resistance determined by load tests for piles driven in sand.

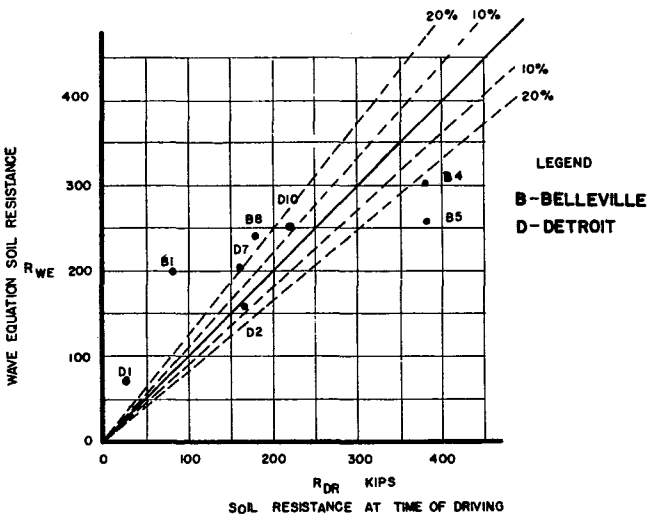

Fig. 10.2. Comparison of wave equation soil resistance to soil resistance at time of driving estimated from load test results from pile driven in clays.

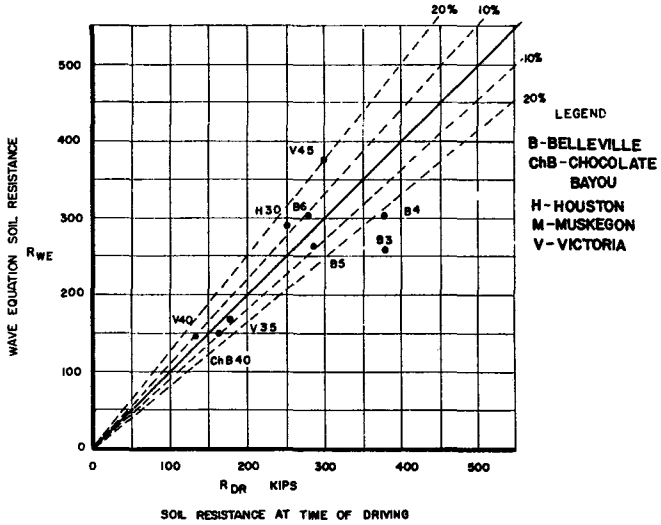

Fig. 10.3. Comparison of wave equation soil resistance to soil resistance at time of driving estimated from load test results from pile driven in sand and clay soils.

(R_{WE}) with the soil resistance at the time of driving (R_{dr}) as estimated from the load test results on piles supported both by "SANDS" and "CLAYS." Data presented in this figure were obtained from Table 9.3. The average accuracy of the wave equation prediction was approximately $\pm 15\%$.

The comparisons shown in Fig. 10.1, 10.2, and 10.3 were obtained by using the following typical soil parameters in Eq. 6.

TABLE 10.1. TYPICAL SOIL PARAMETERS

SOIL TYPE	Q in.	$J_{(p)}$ sec/ft	$J_{(m)}$ sec/ft
SANDS	0.10	0.10	0.033
CLAYS	0.10	0.30	0.100

It should be kept in mind that for piles driven in clays, the actual load test results (R_{LT}) will be somewhat higher than the soil resistance at the time of driving (R_{dr}) because of the influence of soil "set-up" or reconsolidation of the soil.

Chapter XI

CONCLUSIONS

This report has shown how the wave equation analysis of the dynamic behavior of piling during driving can be used to predict or estimate a pile's load bearing capacity. While driving piles in the field, the pile penetration or permanent set per blow can be observed and this can be translated into the soil resistance acting on the pile at the time of driving if all other variables are known. For a given pile, driving equipment, and foundation conditions the wave equation method can be used to generate a curve relating blows per inch to the total soil resistance acting on the pile during driving. It is again emphasized that this soil resistance is the soil resistance encountered by the pile during driving. To translate this soil resistance at the time of driving to load bearing capacity, the time effect or soil "set-up" which usually tends to increase the pile bearing capacity will have to be considered. If the soil resistance is predominantly due to cohesionless materials such as sands and gravels, the time effect or soil "set-up" tending to increase the pile bearing capacity will usually be small or negligible. On the other hand, if the soil is a cohesive clay, the time effect or soil "set-up" might increase the bearing capacity as discussed in Chapter IV. The magnitude of this "set-up" can be estimated if the sensitivity and reconsolidation properties of the clay are known. It can also be conservatively disregarded since the "set-up" bearing capacity is usually greater than that predicted by this wave equation method.

The accuracy of this method is primarily dependent upon making reasonable assumptions for the following soil parameters which are used to describe its behavior in this dynamic analysis. These soil parameters are as follows:

1. Distribution of the soil resistance along the pile (percent of total soil resistance acting on the point and percent of total soil resistance acting in friction along the side of the pile).

2. Soil Quake "Q" (soil quake is the elastic deformation of the soil medium supporting the pile).

3. Soil damping constants "J(p)" and "J(m)".

Small variations in the distribution of the soil resistance between side friction and point bearing will not affect the wave equation results significantly. The soil quake "Q" may range from 0.05 inches to 0.20 inches. The most typical value for average pile driving conditions is 0.10 inches. Values of the soil damping "J(p)"

and "J(m)" have a significant effect on the wave equation results. For the best correlation between the wave equation predicted soil resistance and the soil resistance acting on the pile at the time of driving as determined from load tests, the typical value of J(p) for sands was found to be 0.1. For the best correlation with piles driven in clays a typical value of J(p) was found to be 0.3. In all cases J(m) was assumed to be ⅓ of J(p).

Using these values of soil damping and quake a "reasonable" correlation between the wave equation solution and full-scale load tests was found. The average accuracy of the wave equation prediction of the load capacity at the time of driving was approximately ±25% for piles supported only in sands. The average accuracy of the wave equation prediction of the load capacity at the time of driving was approximately ±40% for piles supported entirely by clays. The average accuracy of the wave equation prediction of load capacity at the time of driving for piles supported by both sandy and clay soils was approximately ±15%.

While the accuracy of the correlations presented here are not as good as one might hope for, this method of analysis is believed to be far superior to any other dynamic method now available. The accuracy of the wave equation method of predicting soil resistance on a pile at the time of driving appears, at this time, to be quite good for piles driven in sands and sandy soils. It is also apparent that the accuracy of this method of predicting soil resistance on a pile during driving in clays is not as accurate, at this time, as for piles driven in sands. One should bear in mind, however, the extremely complex nature of clays and cohesive materials.

These conclusions should not be considered as the final word or firm. They are only intended to define the "state of the art" for using the wave equation to predict pile load bearing capacity.

References

1. Chellis, R. D., *Pile Foundations*, McGraw-Hill Book Company, New York, 1951, p. 30.
2. Cummings, A. E., "Dynamic Pile Driving Formulas," *Journal of Boston Society of Civil Engineers*, January, 1940.
3. Smith, E. A. L., "Pile Driving Analysis by the Wave Equation," *Proceedings* ASCE, August, 1960.
4. Smith, E. A. L., "Impact and Longitudinal Wave Transmission," *Transactions*, ASME, August, 1955.
5. Smith, E. A. L., "What Happens When Hammer Hits Pile," *Engineering News Record*, September 5, 1957.
6. Smith, E. A. L., "Tension in Concrete Piles During Driving," *Journal of Prestressed Concrete Instruments*, Vol. 5, 1960.
7. Samson, C. H., T. J. Hirsch, and L. L. Lowery, Jr., "Computer Study of Dynamic Behavior of Piling," *Journal of the Structural Division*, ASCE, Vol. 89, No. ST4, Proceedings Paper 3608, August, 1963.
8. Lowery, L. L., Jr., T. J. Hirsch, and C. H. Samson, Jr., "Pile Driving Analysis—Simulation of Hammers, Piles, and Soils," Report of the Texas Transportation Institute, Texas A&M University, September, 1967.
9. Chellis, R. D., *Pile Foundations*, McGraw-Hill Book Company, New York, 1951, p. 506.
10. Forehand, P. W., and J. L. Reese, "Pile Driving Analysis Using the Wave Equation," Master of Science in Engineering Thesis, Princeton University, 1963.
11. Michigan State Highway Commission, "A Performance Investigation of Pile Driving Hammers and Piles," Office of Testing and Research, Lansing, Michigan, March, 1965.
12. Ibid., p. 209.
13. Ibid., p. 246.
14. Mansur, C. I., "Pile Driving and Loading Tests," Presented at ASCE Convention in New York, New York, October 22, 1964.

Appendix A

INSTRUMENTATION OF TEXAS GULF COAST LOAD TEST PILES

EMBEDDED STRAIN GAGES

Selection of Gages

Two types of gages were used in the pile instrumented in this research. Early in the program a foil-encased gage manufactured by the Baldwin Co. was used. Limited data were obtained due to the failure of many of the gage installations due to loss of resistance to ground. Whether this was due to moisture leakage at the gage is not known, but the trouble consistently caused the loss of at least one gage installation in each pile, and in several cases every gage was lost.

A second type of gage was used to instrument the remainder of the piles. This was a polyester mold gage, consisting of a standard 300 ohm gage hermetically sealed between two polyester blocks. This encapsulation completely waterproofs both the gage and lead wires, and provided an extremely tough protective shell which simplified installation greatly. The faces of the blocks are coated with a sand grit to insure proper bond with the concrete of the pile whereas the foil-encased gage was susceptible to bond failure. These gages proved completely reliable in every respect, and no further failures were experienced, even though many of the piles were driven below the water line and were not load-tested for several months.

The physical characteristics of a typical gage are as follows:

Gage length = 100 mm
Gage width = 3 mm
Nominal resistance = 300 ohms
Maximum admissible current = 35 ma
Gage factor = 2.19
Block dimensions = 170 × 13 × 5 mm

Figure A.1 shows a photograph of this type of gage.

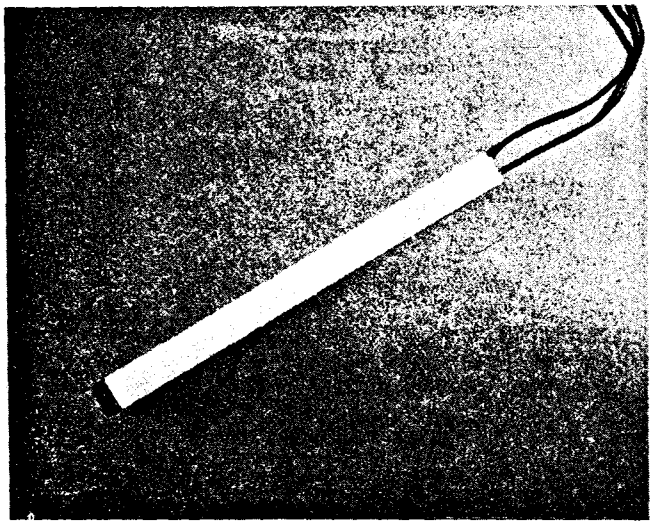

Fig. A.1. Typical strain gage used to instrument a majority of the piles in the research.

Electrical Circuit and Recording Instrumentation

Each gage point in the pile consisted of four gages arranged in a Wheatstone bridge. The active gages were loosely taped to the reinforcing strands parallel to the longitudinal axis of the pile and diametrically opposite each other to eliminate bending stresses. The dummy gages were placed at right angles to the active gages and diametrically opposite each other. A wiring diagram of the bridge circuit and the physical layout is shown in Fig. A.2.

Each bridge was powered by a 5 volt, 5 kc alternating current. The bridge output was amplified and recorded on a recording oscillograph. The power supply, amplifiers and recording equipment used in this research were as follows:

Power Supply and Amplifiers—Honeywell Model 119

Recording Oscillograph—Honeywell Model 1508 Visicorder

Galvanometers—Honeywell Model M-1650 fluid damped.

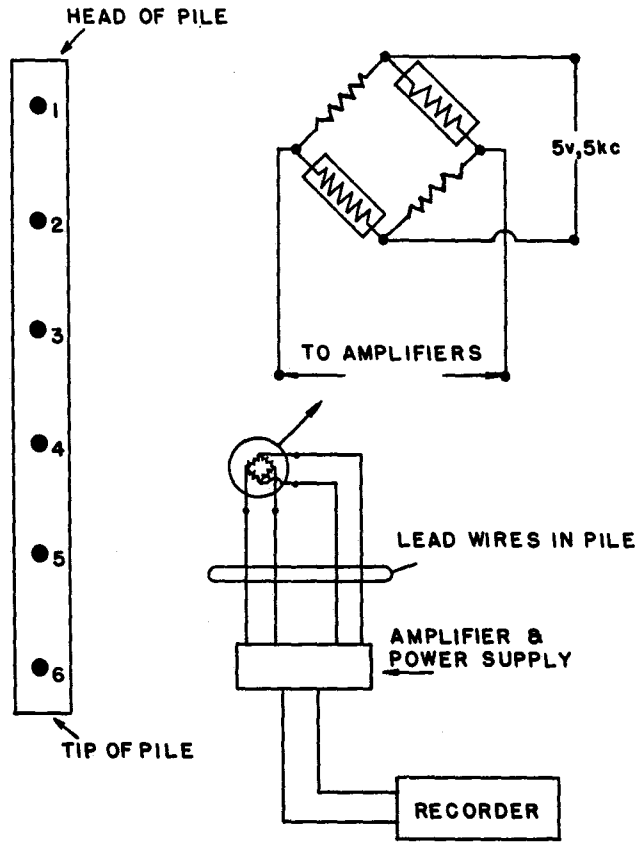

Fig. A.2. Wiring diagram.

Installation of Gages

Since this research was concerned primarily with the measurement of stresses, electric resistance strain gages were chosen as the primary instrumentation. Problems inherent with the use of strain gages are magnified when they are used under field conditions.

The instrumentation of prestressed piling for field use presented many problems. Fig. A.3 shows a sketch of a typical gage point installation. Since the gage connections and lead wires were to be cast in the pile, adequate moisture protection during manufacture of the pile was imperative. The entire system also had to be protected from moisture until the pile was driven, and subsequently from the time of driving until the static load test was run. The gages themselves had to be installed in such a manner that they would not be damaged during the manufacture of the pile. It was found that the mold gage itself required no additional waterproofing, and that it was sufficiently strong to withstand the placing and vibrating of the concrete without being damaged.

Each gage point was pre-fabricated in the laboratory, and consisted of a completely waterproof module including the gage bridge, main lead wires, and surface connectors. This module scheme permitted fast field installation with a minimum of interference to the pile fabricator. Each module could also be tested, zeroed, balanced, etc., before leaving for the job site.

The main lead cables were laid along the upper surface of the pile and secured to the reinforcing strands at frequent intervals with plastic tape. Care was taken to insure that the main lead cables were not placed in one bundle but were spread uniformly across the surface. Otherwise, considerable crosstalk between channels may result. At the head of the pile the main lead cables were bundled and wrapped with plastic tape to form a common exit. Approximately 10 ft of lead cable was left exposed at the head of the pile, the connection having earlier been completely waterproofed by potting

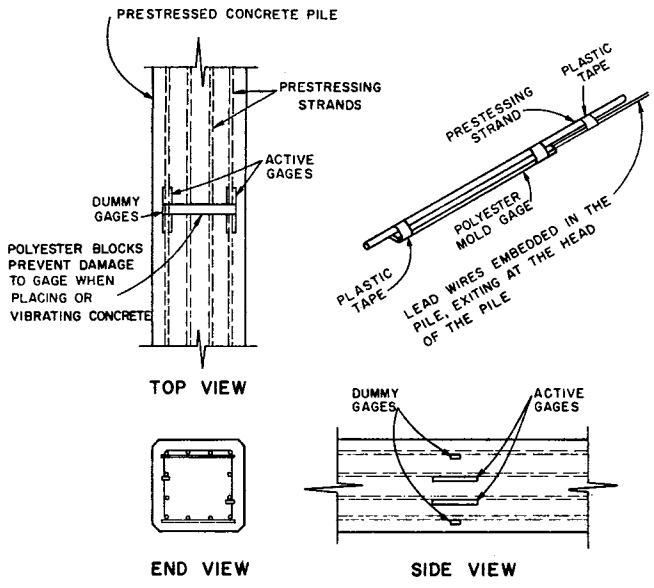

Fig. A.3. Typical gage installation.

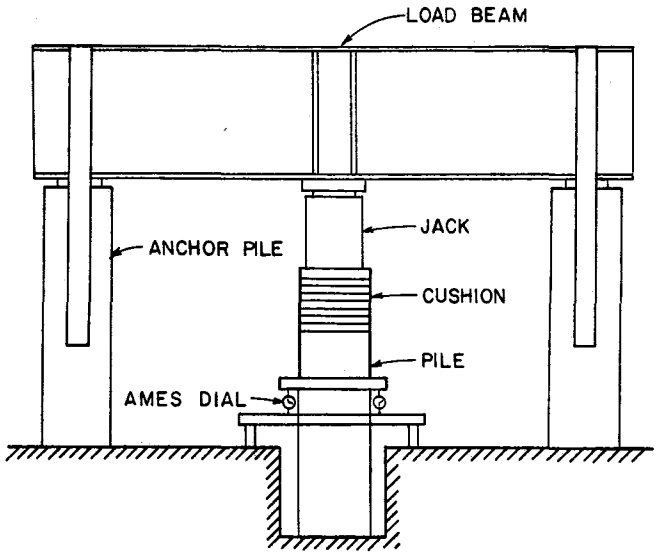

Fig. A.4. Load test fixture.

with RTV silicone rubber. This potting compound was completely reliable and was easily cut off the connectors immediately prior to testing. After testing, the connectors were again potted for possible future use.

Calibration of Gages

Due to the nature of the gage installation it was not practical to calibrate the bridge by loading; it was decided to use a shunt resistor to simulate strain results.

In this method one active arm of the bridge is shunted by a known resistance. This causes a change in resistance in the active arm and in effect simulates strain. The simulated strain can be determined from the following relation:

$$\epsilon_s = \frac{R_g}{(GF)\ (N)\ (1 + \mu)\ (R_g + R_c)} \qquad \text{Eq. A.1}$$

where

R_g = gage resistance in ohms
GF = gage factor
N = number of active gages
μ = Poisson's ratio
R_c = shunt resistance in ohms
ϵ_s = simulated strain in inch/inch

Load Test Fixtures

Fig. A.4 shows a typical load test fixture used on these tests. The fixture consists essentially of a loading beam and an arrangement of anchor piles. The thrust of the jack is transmitted by the load beam to the anchors. The basic fixtures used in the tests in this report were the same; however, various types of loading beams and anchor systems were used at each site.

In each test, load was applied with a 200-ton capacity hydraulic jack. A wood cushion (6 to 8 inches of plywood) was placed between the jack and the head of the pile and dial gages were attached to the pile to measure displacements.

Test Procedure

All main lead wires from the gages were connected to the power supply and amplifiers. Each bridge was balanced before the load was applied. The first increment of load of 5 tons was placed on the pile and held constant for 2½ minutes. During this time, strains were recorded as well as at the beginning and end of the 2½ minute waiting period. The pile was progressively loaded in 5-ton increments until excessive penetration denoted failure or the capacity of the equipment was reached. Data were recorded at each load increment according to the outline above.

Data Reduction

The load distribution curves shown in Chapter VII were derived using the recorded strain readings at the indicated loads. The force in the pile at any gage point is a function of the strain, modulus of elasticity of the pile material and the cross-sectional area of the pile. This force is given by:

$$F_i = \epsilon_i E_i A_i \qquad \text{Eq. A.2}$$

where

F_i = force in the pile at gage point i,

ϵ_i = strain at gage point i in inch/inch,

E_i = modulus of elasticity of the pile material at gage point i, and

A_i = cross-sectional area of the pile at point i.

The constant E_iA_i was determined by using the data from the head gage point which was located 1 ft from the head of the pile. This gage point was always free from side soil friction and hence could be correlated with the applied load at the head of the pile. With F_1 known, the required constants can be determined from:

$$E_1A_1 = \frac{F_1}{\epsilon_1} \qquad \text{Eq. A.3}$$

Assuming that E and A are constant throughout, the force at any point in the pile can be found by:

$$F_i = \left(\frac{F_1}{\epsilon_1}\right)\epsilon_i \qquad \text{Eq. A.4}$$

Appendix B

PILE LOAD-TRANSFER CURVES
FIGURES B.1 THRU B.22

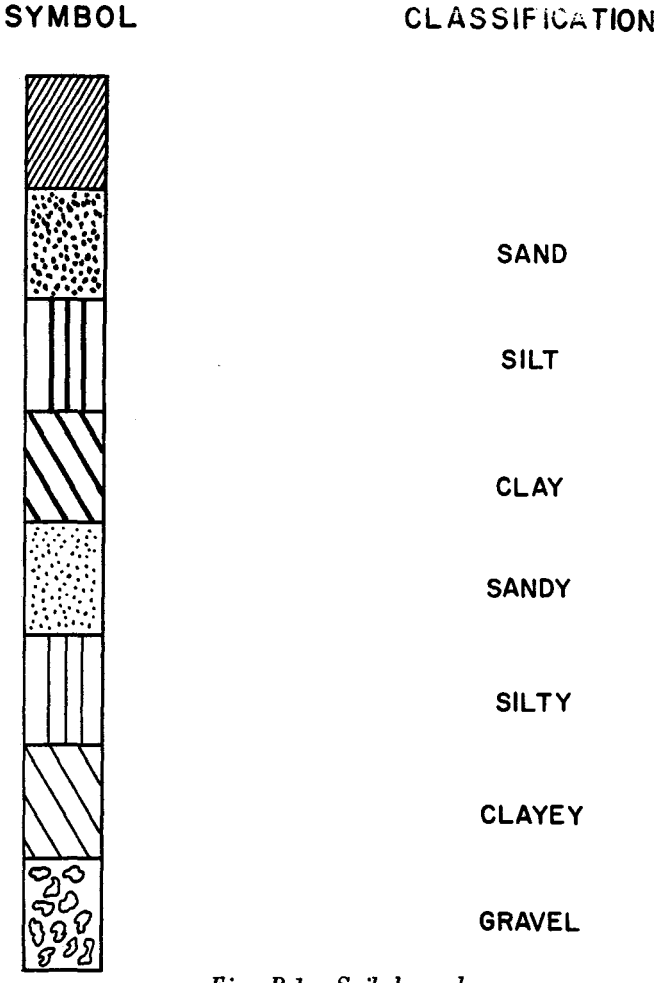

Fig. B.1. Soil legend.

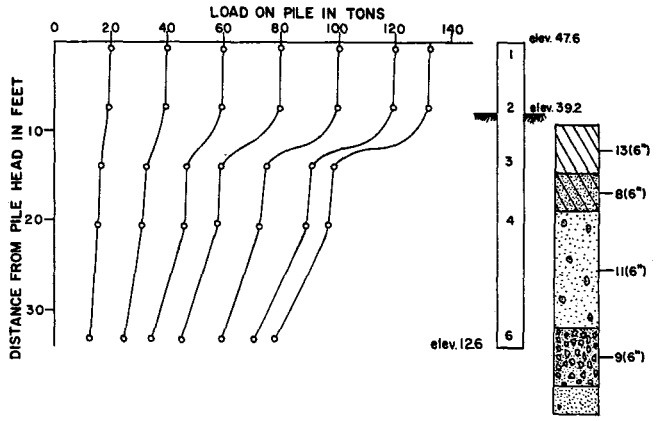

Fig. B.2. Pile load distribution for Victoria Bridge, 35-foot pile.

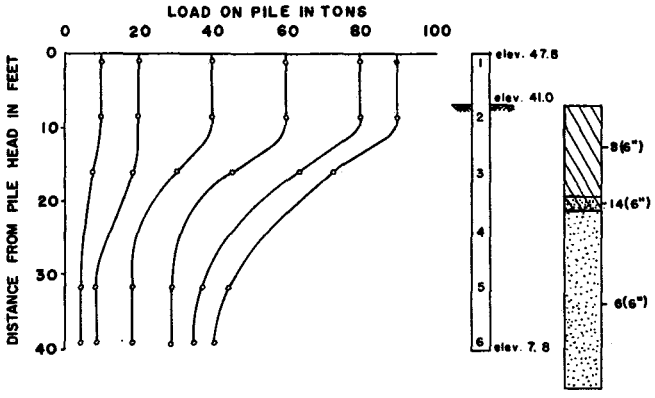

Fig. B.3. Pile load distribution for Victoria Bridge, 40-foot pile.

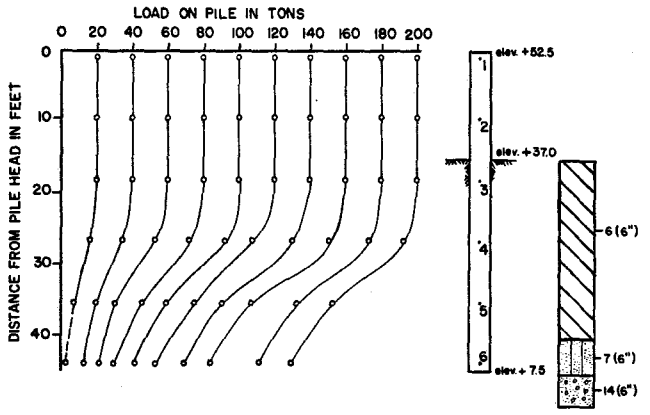

Fig. B.4. Pile load distribution for Victoria Bridge, 45-foot pile.

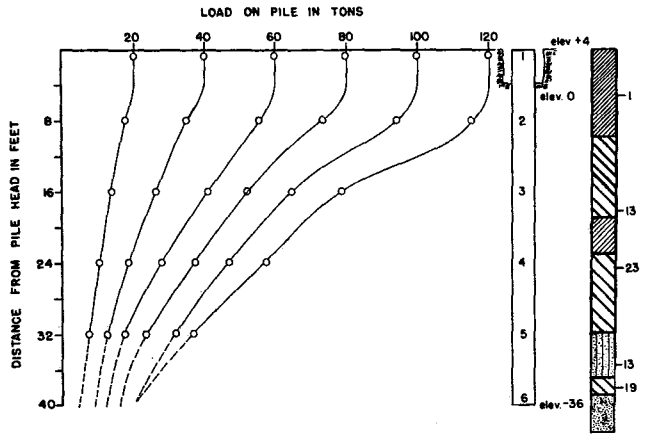

Fig. B.5. Pile load distribution for Chocolate Bayou Bridge, 40-foot pile.

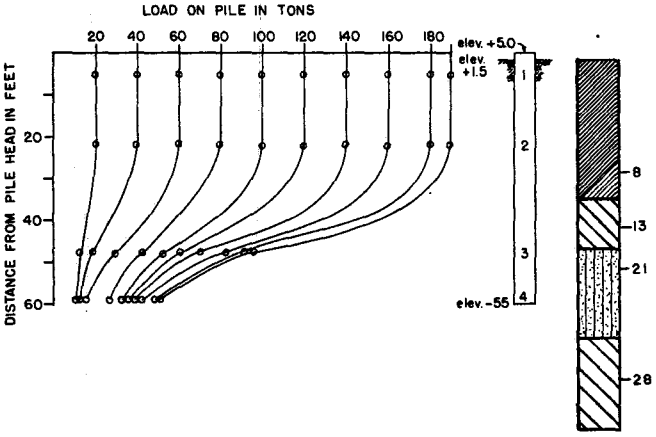

Fig. B.6. Pile load distribution for Chocolate Bayou Bridge, 60-foot pile.

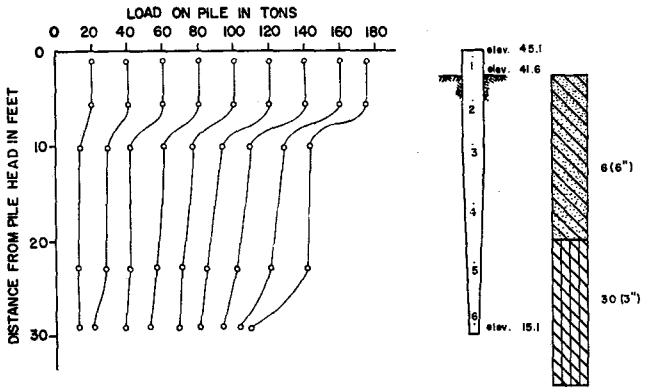

Fig. B.7. Pile load distribution for Houston, 30-foot tapered pile.

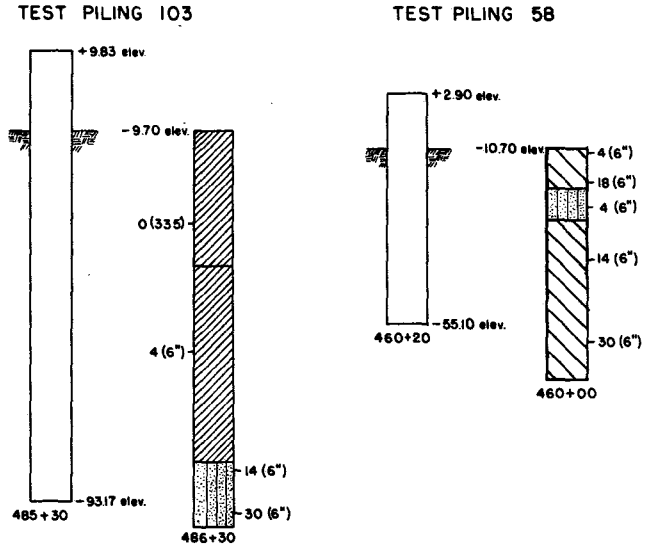

Fig. B.8. Soil profile for Copano Bay Bridge Load Test Piles 58 and 103.

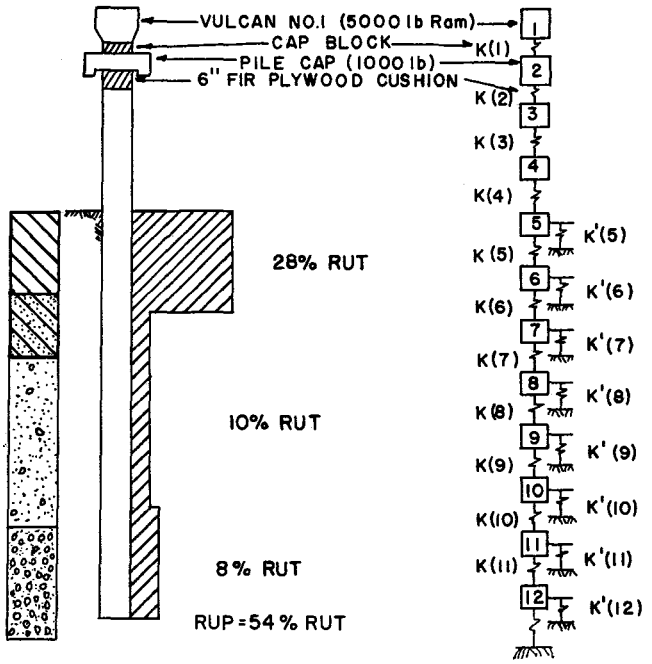

Fig. B.9. Idealization of pile for purpose of computer analysis, Victoria Bridge, 35-foot pile.

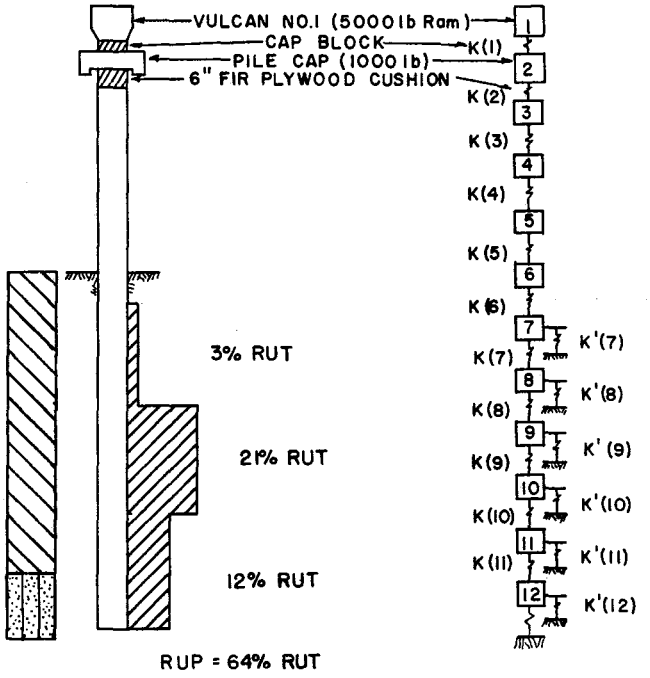

Fig. B.11. Idealization of pile for purpose of computer analysis, Victoria Bridge, 45-foot pile.

VICTORIA BRIDGE 40 FT PILE

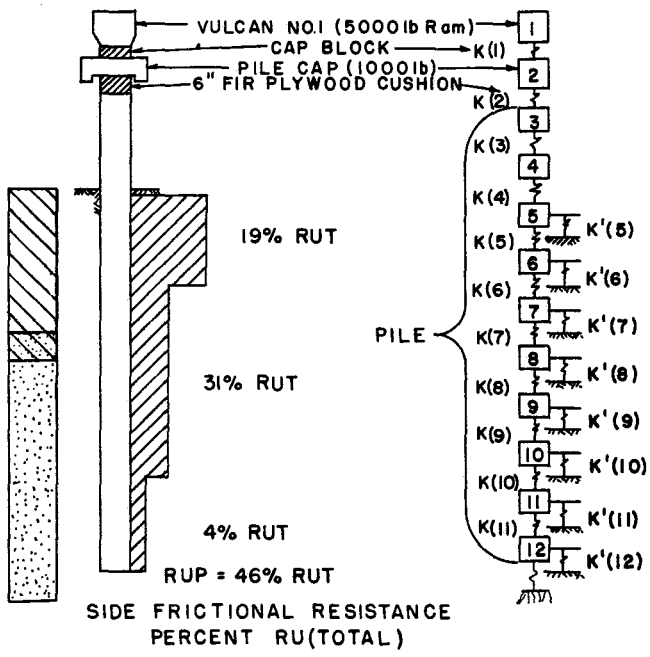

Fig. B.10. Idealization of pile for purpose of computer analysis, Victoria Bridge, 40-foot pile.

CHOCOLATE BAYOU 40 FT PILE

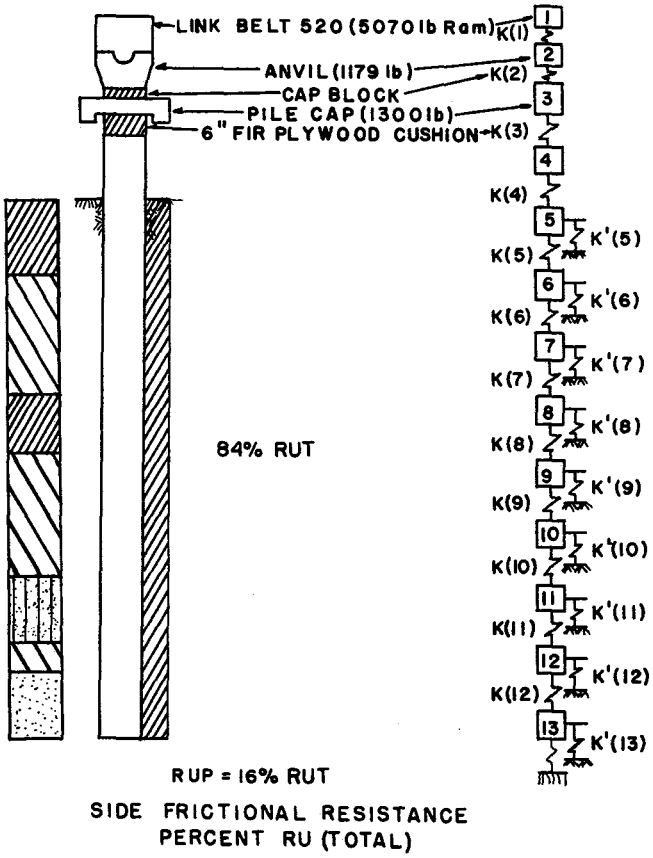

Fig. B.12. Idealization of pile for purpose of computer analysis, Chocolate Bayou Bridge, 40-foot pile.

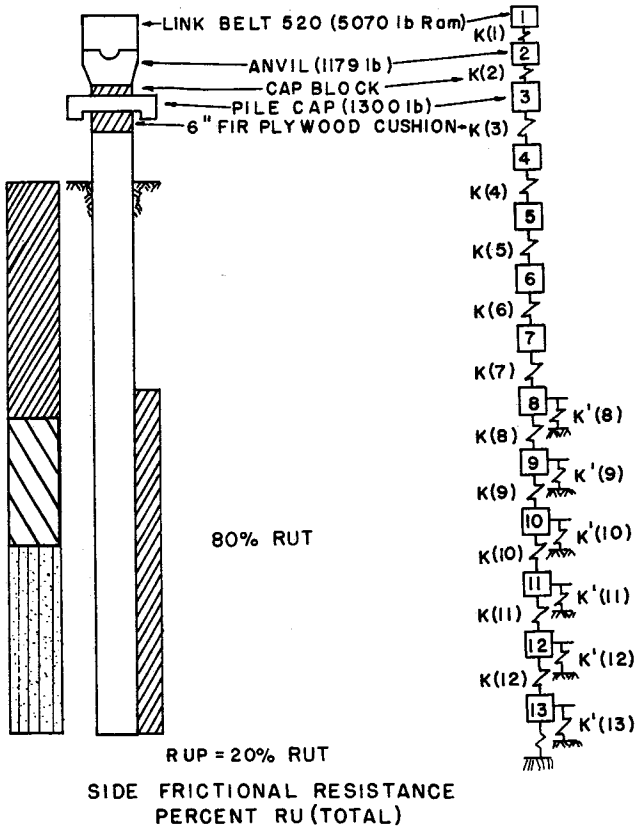

Fig. B.13. Idealization of pile for purpose of computer analysis, Chocolate Bayou Bridge, 60-foot pile.

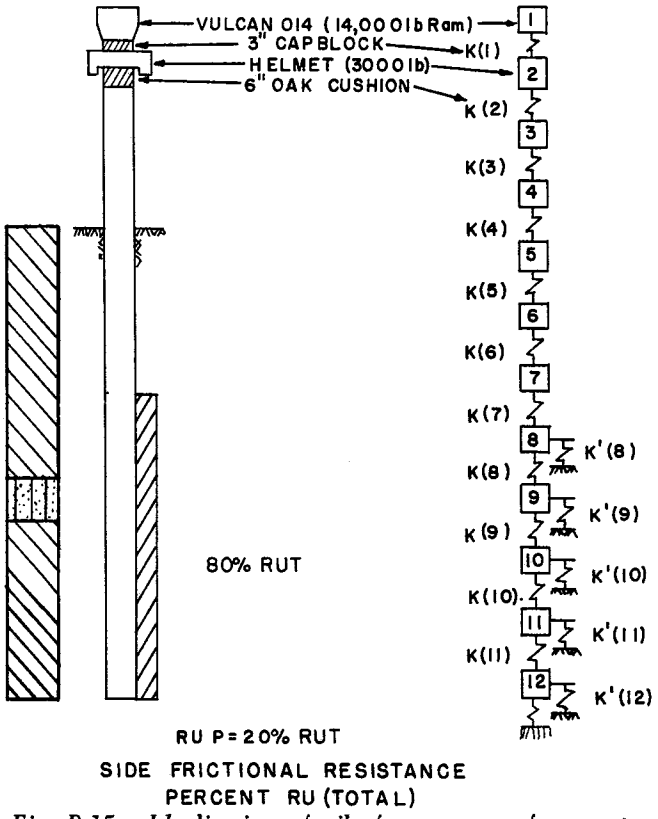

Fig. B.15. Idealization of pile for purpose of computer analysis, Copano Bay, 58-foot pile.

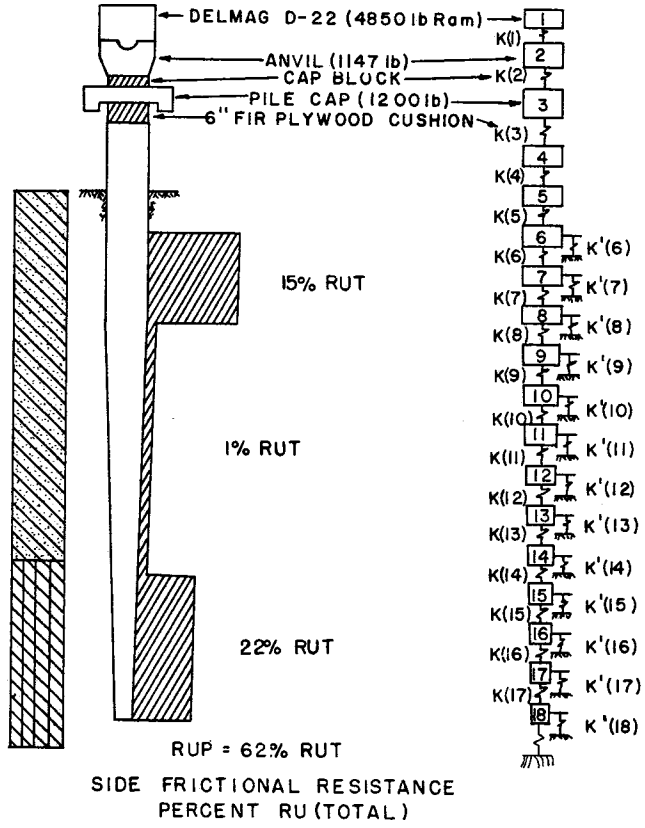

Fig. B.14. Idealization of pile for purpose of computer analysis, Houston, 30-foot tapered pile.

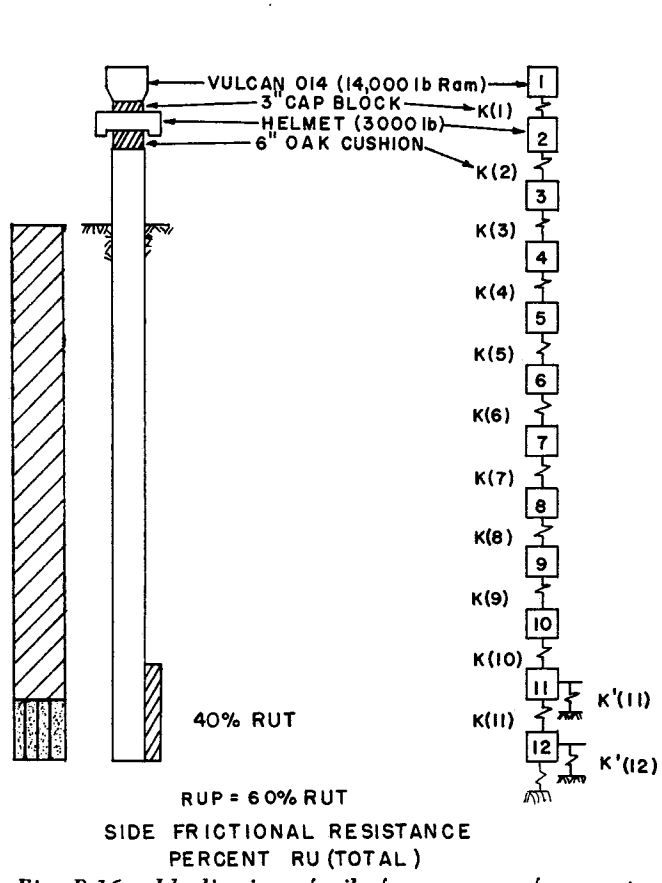

Fig. B.16. Idealization of pile for purpose of computer analysis, Copano Bay, 103-foot pile.

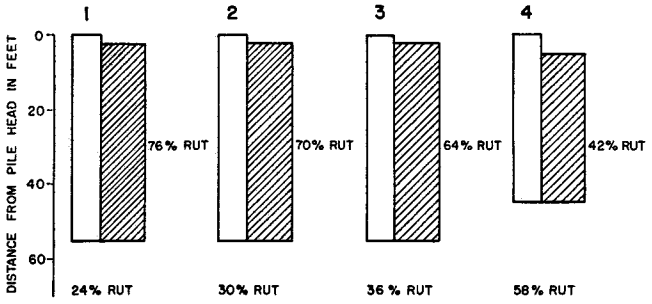

Fig. B.17. Soil resistance distribution for Arkansas Load Test Piles 1, 2, 3, and 4.

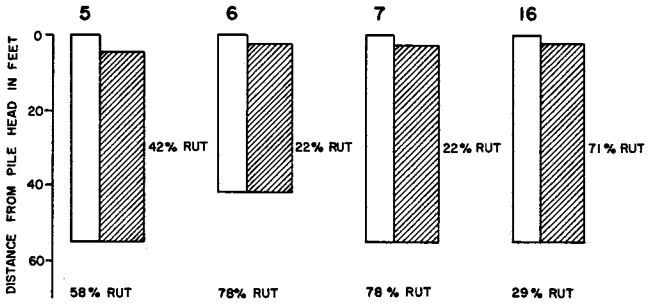

Fig. B.18. Soil resistance distribution for Arkansas Load Test Piles 5, 6, 7, and 16.

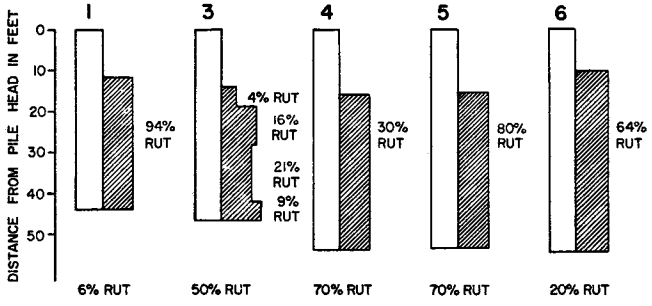

Fig. B.19. Soil resistance distribution for Bellville Load Test Piles 1, 3, 4, 5, and 6.

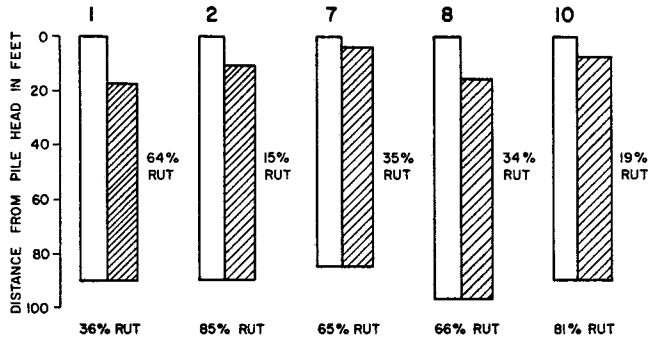

Fig. B.20. Soil resistance distribution for Detroit Load Test Piles 1, 2, 7, 8 and 10.

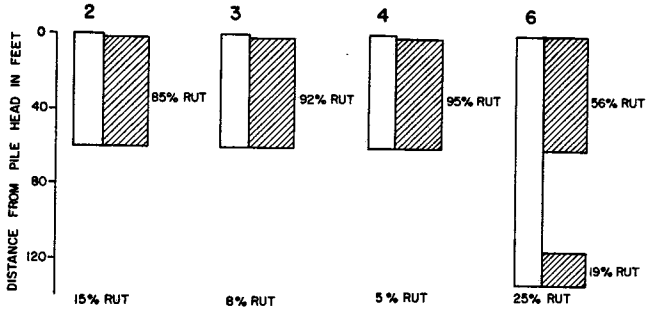

Fig. B.21. Soil resistance distribution for Muskegon Load Test Piles 2, 3, 4, and 6.

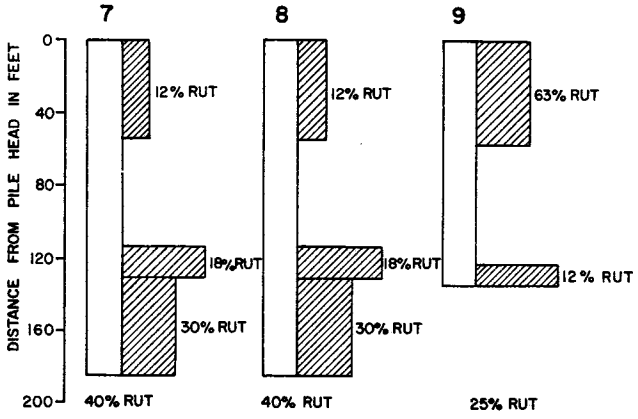

Fig. B.22. Soil resistance distribution for Muskegon Load Test Piles 7, 8, and 9.

Appendix C

LOAD TEST RESULT FOR TEXAS GULF COAST PILES

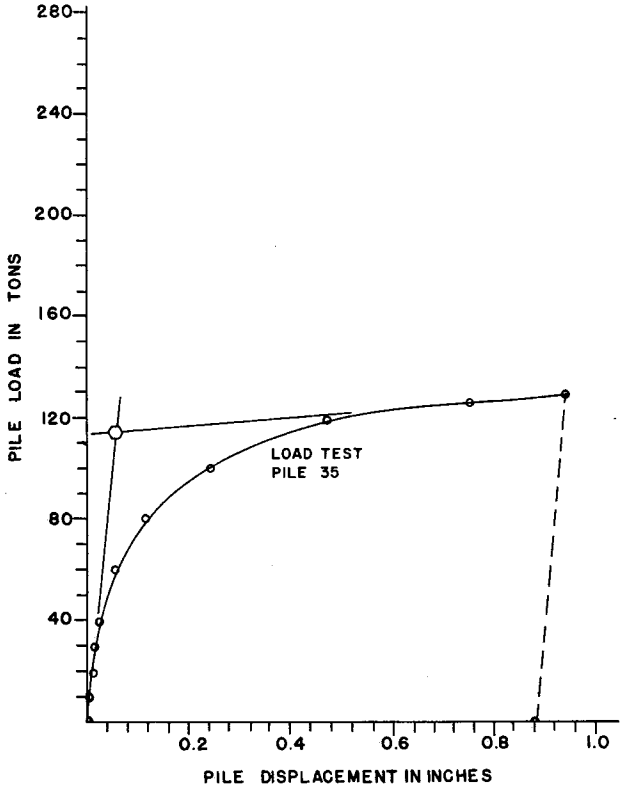

Fig. C.1. Pile load tests for Victoria Bridge Pile 35.

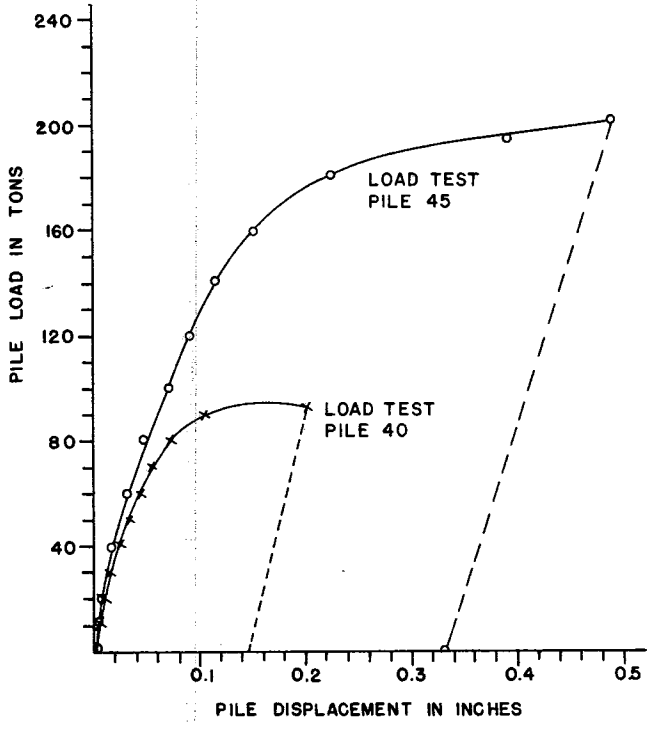

Fig. C.2. Pile load tests for Victoria Bridge Piles 40 and 45.

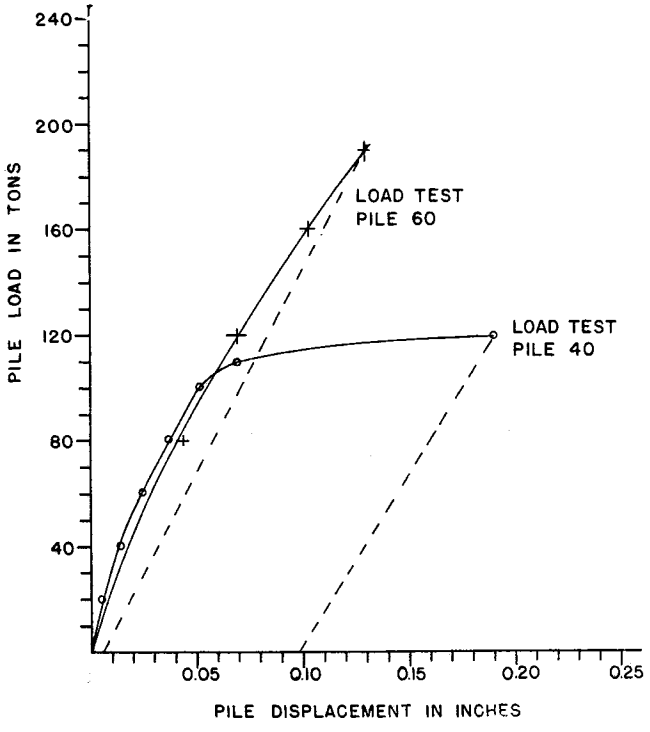

Fig. C.3. Pile load tests for Chocolate Bayou Bridge Piles 40 and 60.

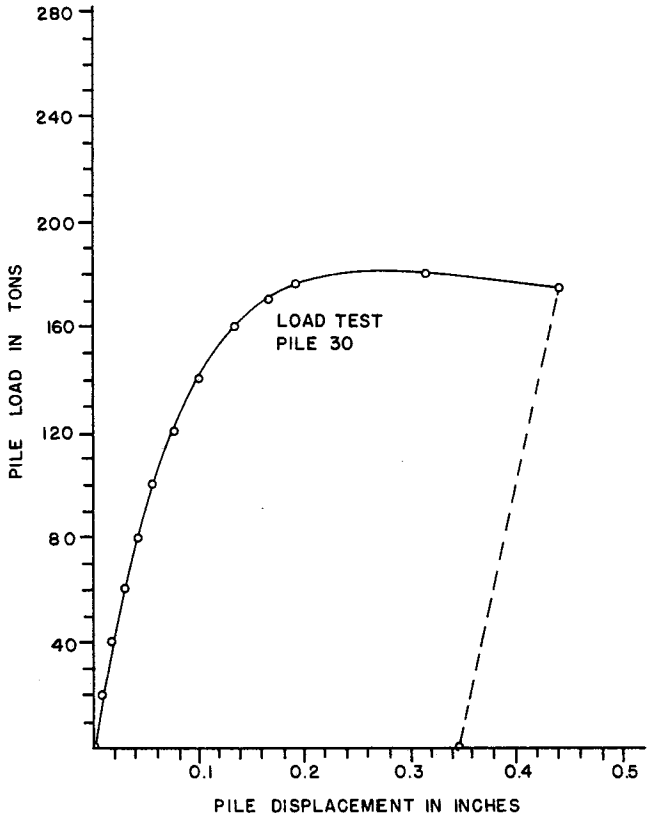

Fig. C.4. Pile load tests for Houston 30 ft tapered pile.

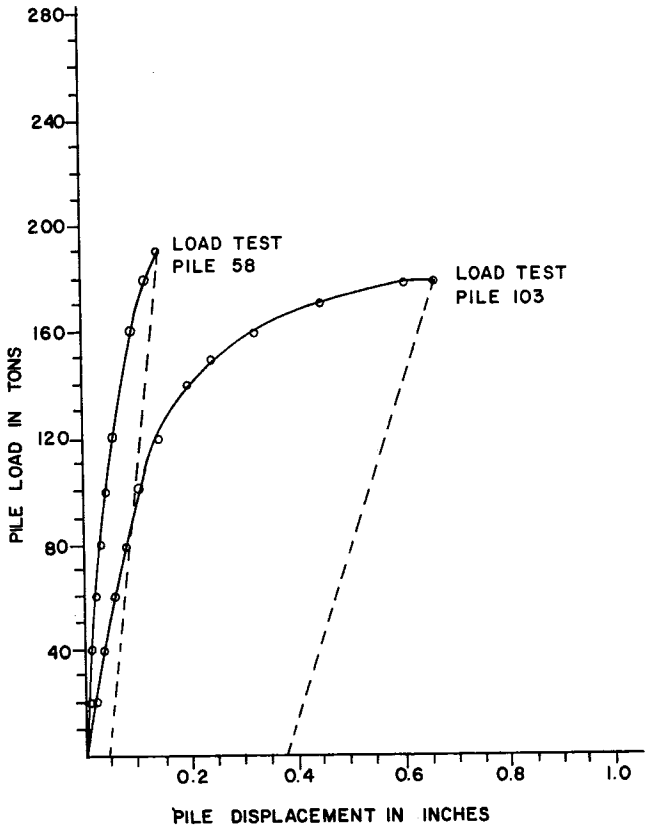

Fig. C.5. Pile load tests for Copano Bay Causeway. Piles 58 and 103.

Appendix D

BLOWS per INCH *VS* RU(total) CURVES FOR TEXAS, ARKANSAS, AND MICHIGAN TEST PILES

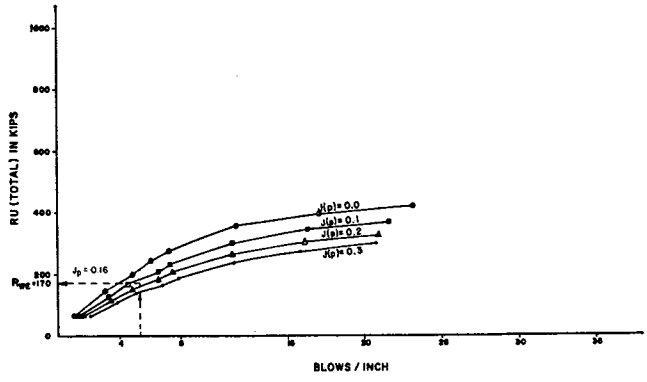

Fig. D.1. Blows/inch vs RU(total) for Victoria Load Test Pile 35.

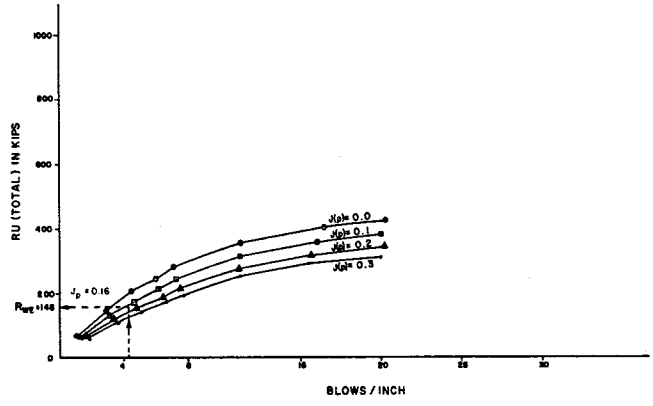

Fig. D.2. Blows/inch vs RU(total) for Victoria Load Test Pile 40.

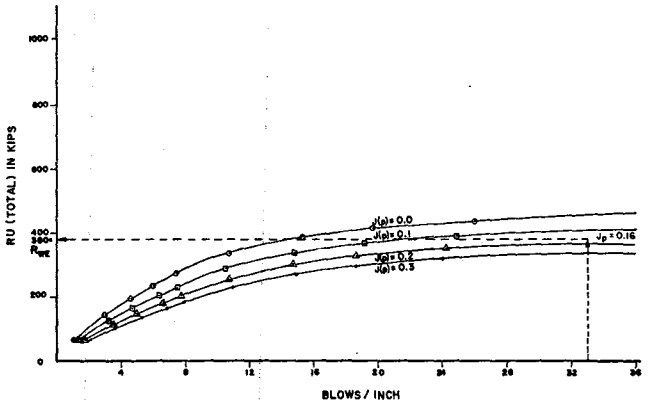

Fig. D.3. Blows/inch vs RU(total) for Victoria Load Test Pile 45.

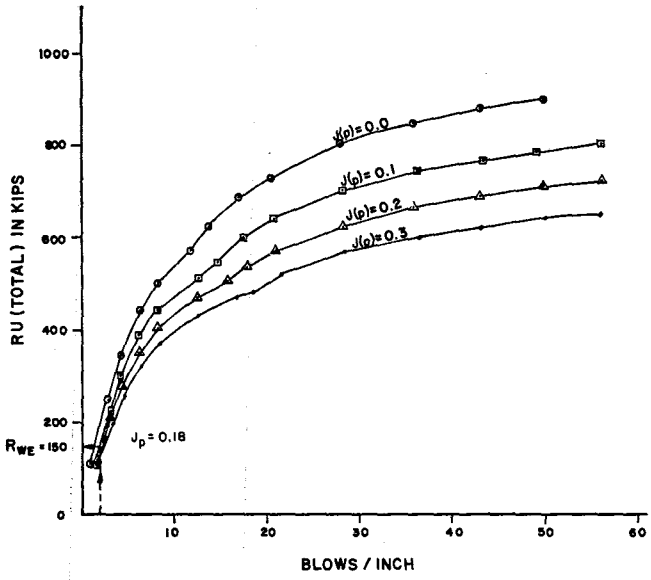

Fig. D.4. Blows/inch vs RU(total) for Chocolate Bayou Load Test Pile 40.

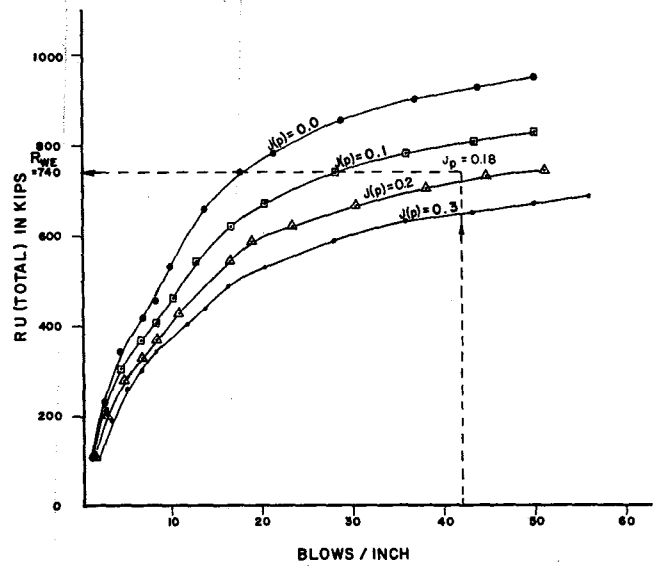

Fig. D.5. Blows/inch vs RU(total) for Chocolate Bayou Load Test Pile 60.

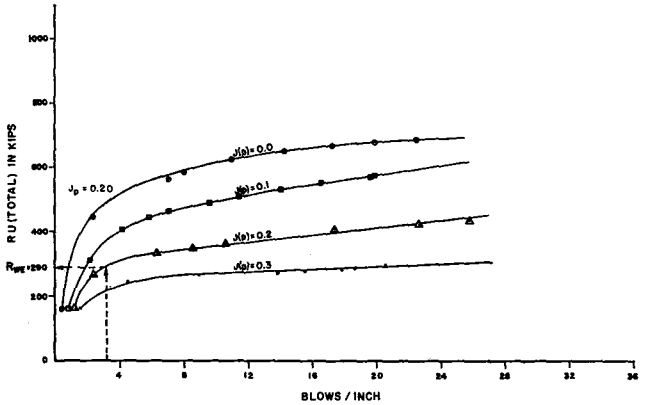

Fig. D.6. Blows/inch vs RU(total) for Houston Load Test Pile 30.

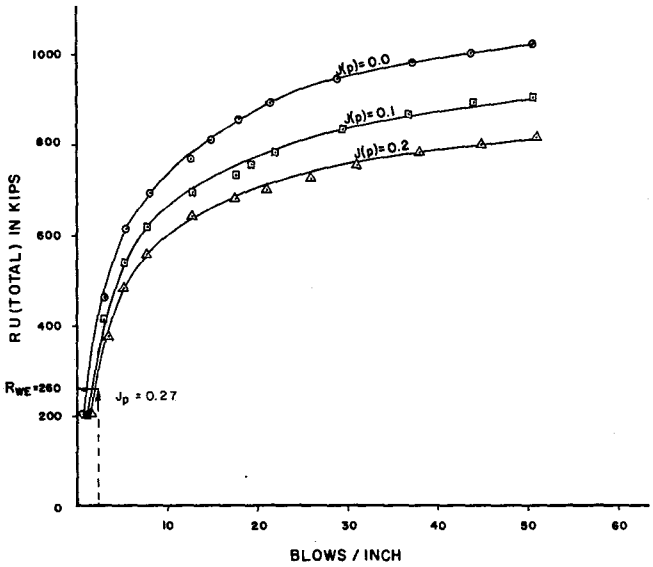

Fig. D.7. Blows/inch vs RU(total) for Copano Bay Load Test Pile 58.

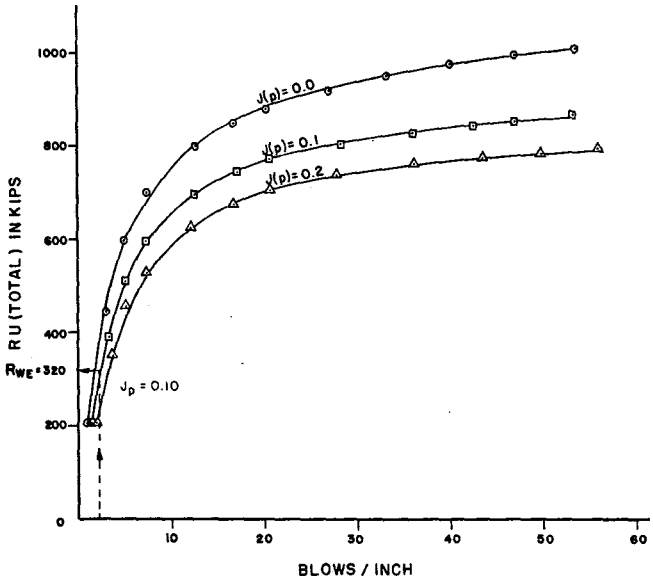

Fig. D.8. Blows/inch vs RU(total) for Copano Bay Load Test Pile 103.

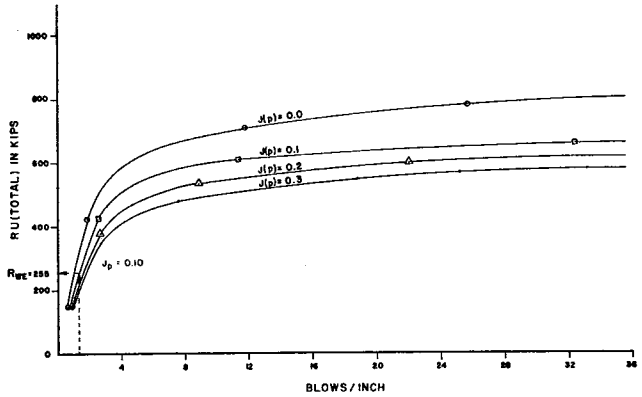

Fig. D-9. Blows/inch vs RU(total) for Arkansas Load Test Pile 1.

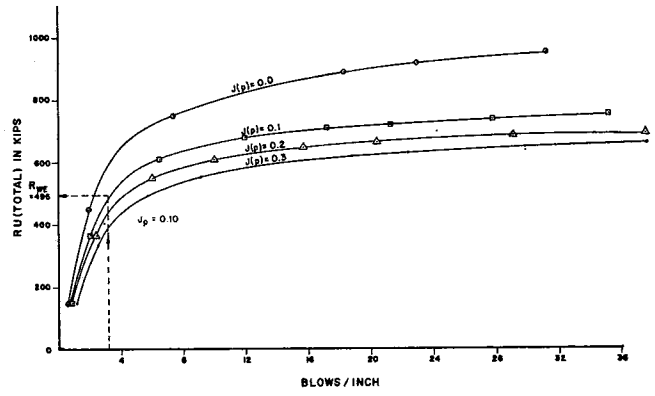

Fig. D.10. Blows/inch vs RU(total) for Arkansas Load Test Pile 2.

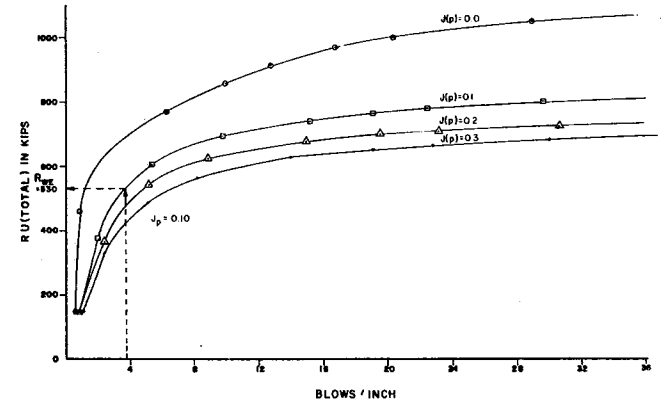

Fig. D.11. Blows/inch vs RU(total) for Arkansas Load Test Pile 3.

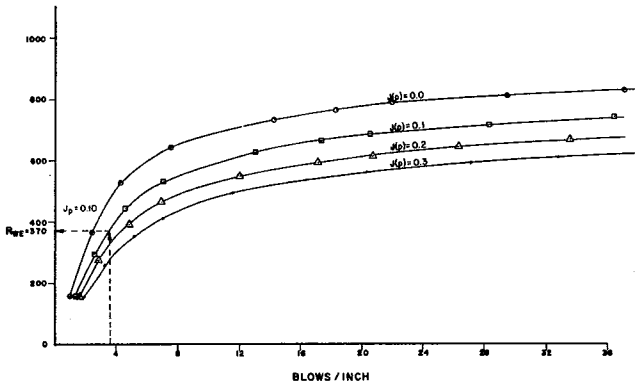

Fig. D.12. Blows/inch vs RU(total) for Arkansas Load Test Pile 4.

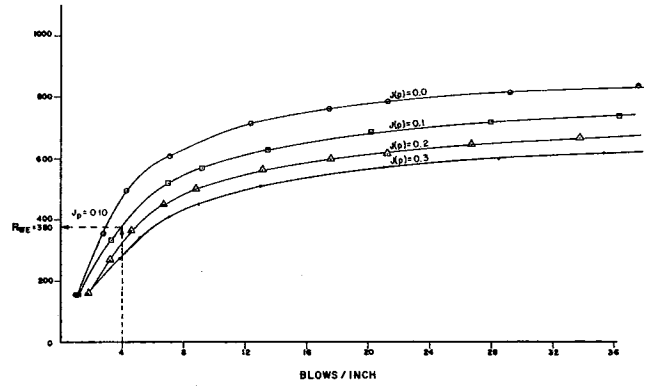

Fig. D.13. Blows/inch vs RU(total) for Arkansas Load Test Pile 5.

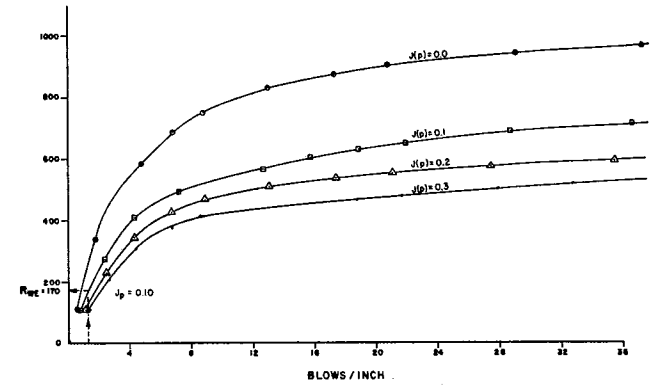

Fig. D.14. Blows/inch vs RU(total) for Arkansas Load Test Pile 6.

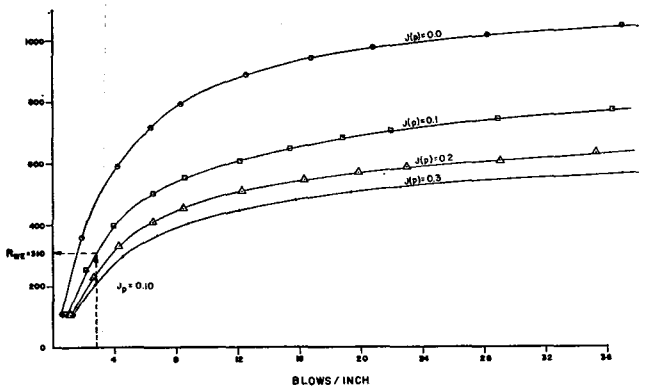

Fig. D.15. Blows/inch vs RU(total) for Arkansas Load Test Pile 7.

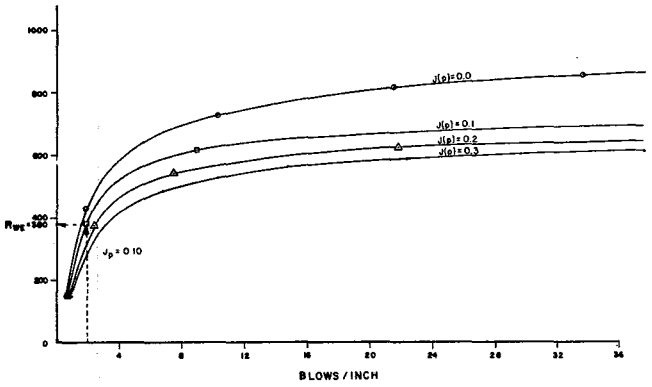

Fig. D.16. Blows/inch vs RU(total) for Arkansas Load Test Pile 16.

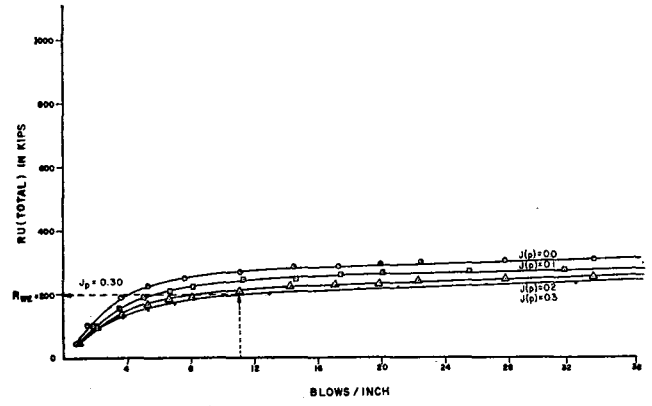

Fig. D.17. Blows/inch vs RU(total) for Belleville Load Test Pile 1.

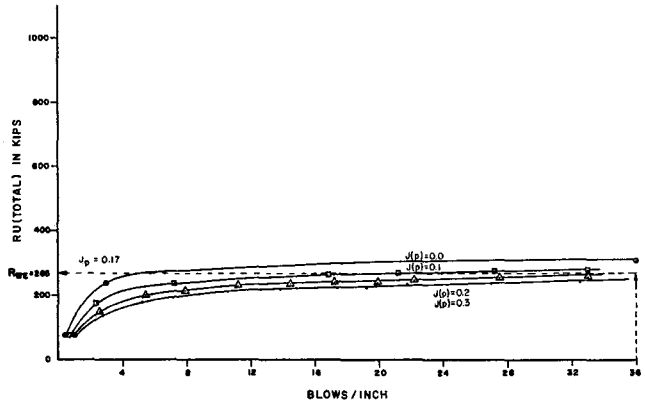

Fig. D.18. Blows/inch vs RU(total) for Belleville Load Test Pile 3.

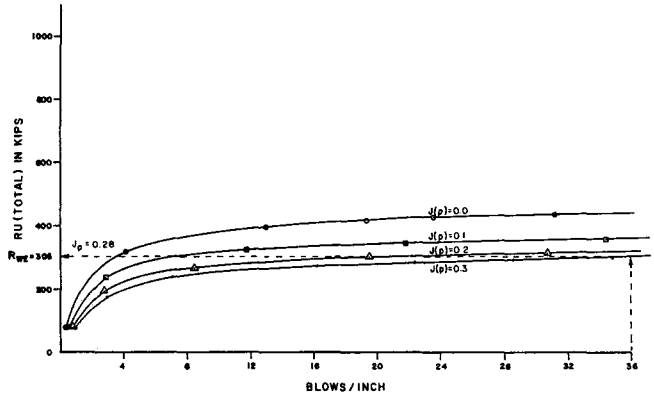

Fig. D.19. Blows/inch vs RU(total) for Belleville Load Test Pile 4.

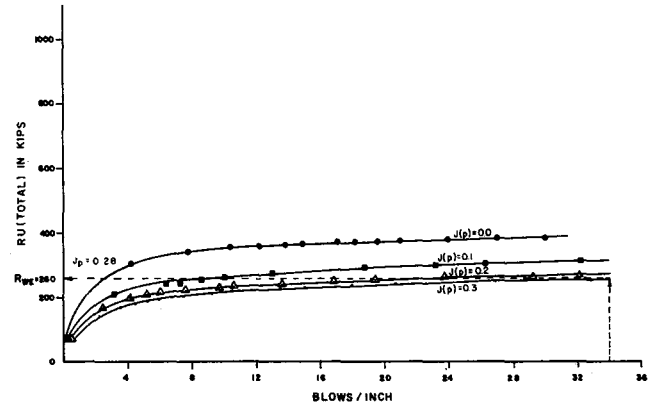

Fig. D.20. Blows/inch vs RU(total) for Belleville Load Test Pile 5.

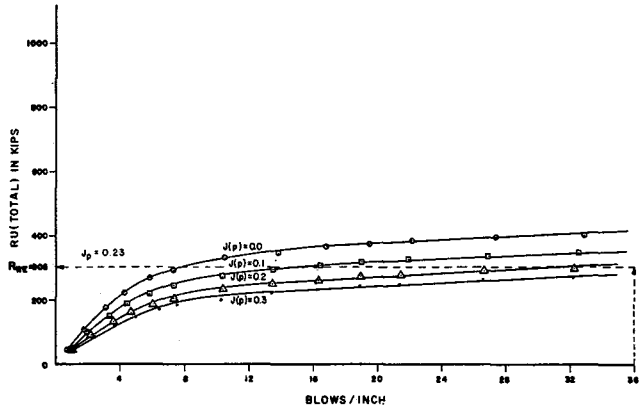

Fig. D.21. Blows/inch vs RU(total) for Belleville Load Test Pile 6.

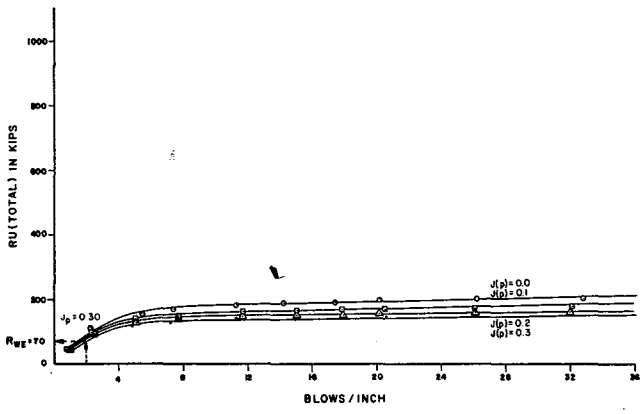

Fig. D.22. Blows/inch vs RU(total) for Detroit Load Test Pile 1.

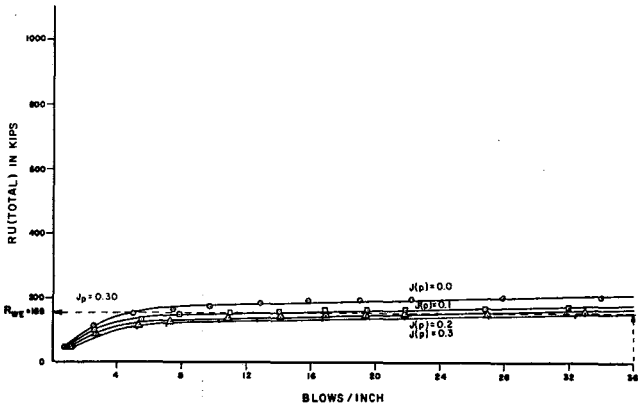

Fig. D.23. Blows/inch vs RU(total) for Detroit Load Test Pile 2.

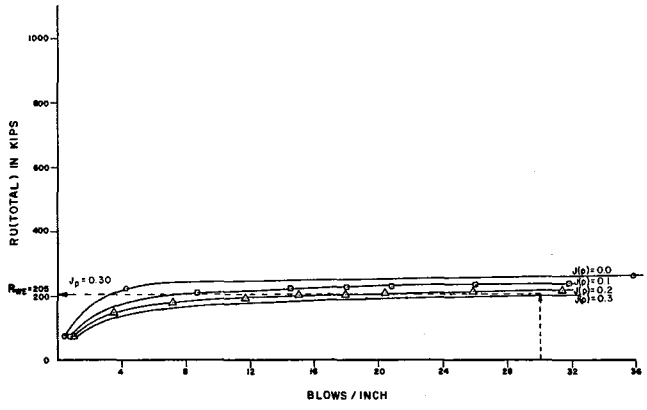

Fig. D.24. Blows/inch vs RU(total) for Detroit Load Test Pile 7.

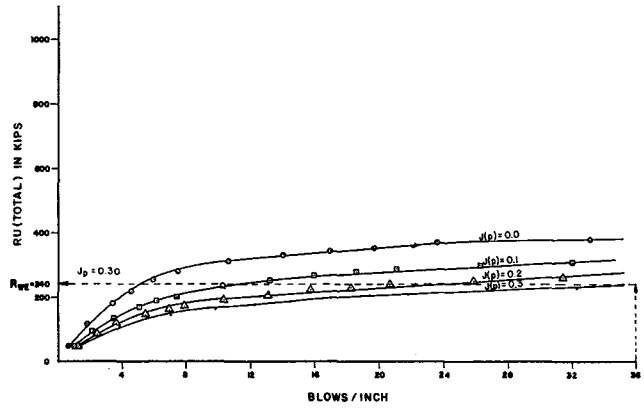

Fig. D.25. Blows/inch vs RU(total) for Detroit Load Test Pile 8.

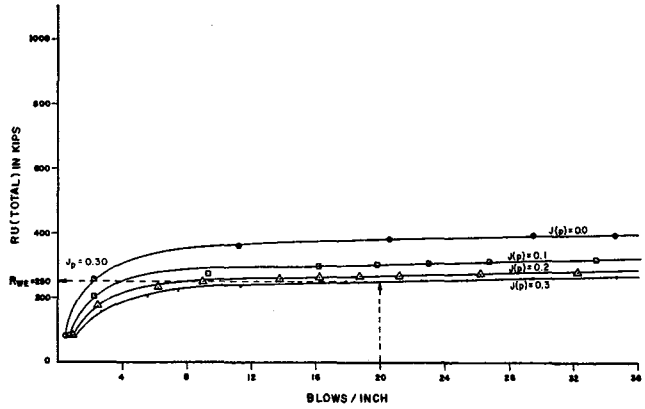

Fig. D.26. Blows/inch vs RU(total) for Detroit Load Test Pile 10.

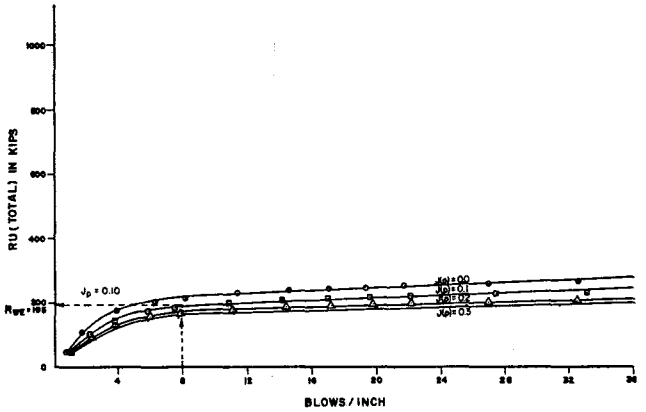

Fig. D.27. Blows/inch vs RU(total) for Muskegon Load Test Pile 2.

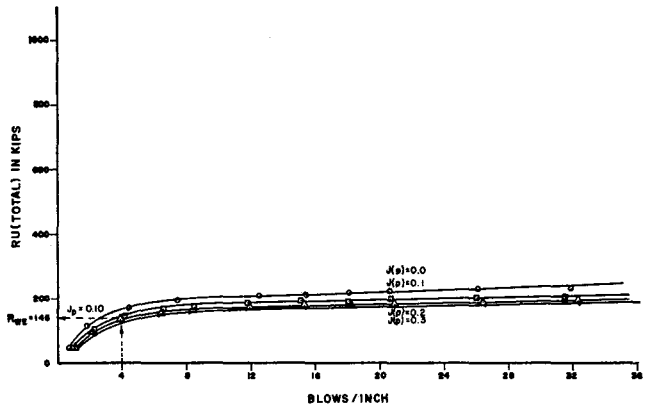

Fig. D.28. Blows/inch vs RU(total) for Muskegon Load Test Pile 3.

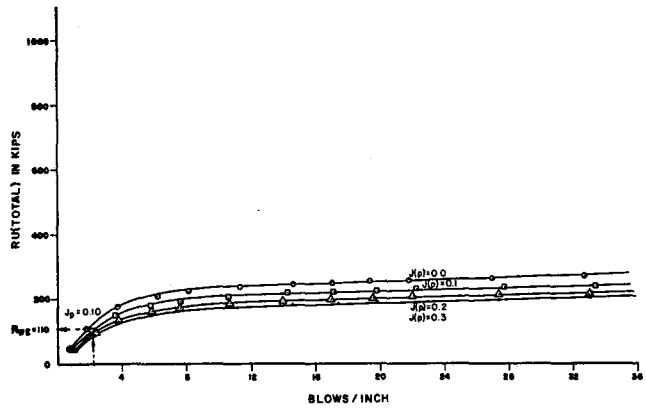

Fig. D.29. Blows/inch vs RU(total) for Muskegon Load Test Pile 4.

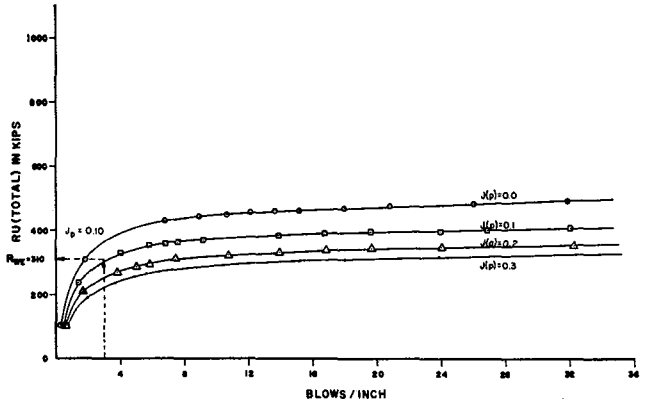

Fig. D.30. Blows/inch vs RU(total) for Muskegon Load Test Pile 6.

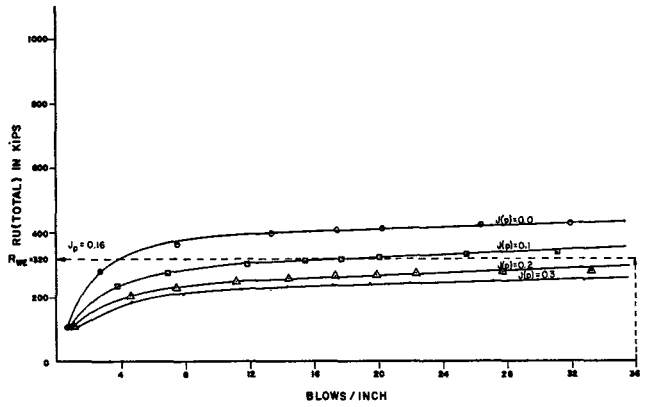

Fig. D.31. Blows/inch vs RU(total) for Muskegon Load Test Pile 7.

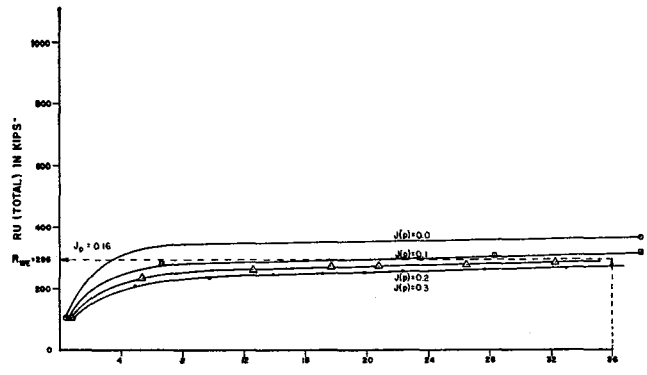

Fig. D.32. Blows/inch vs RU(total) for Muskegon Load Test Pile 8.

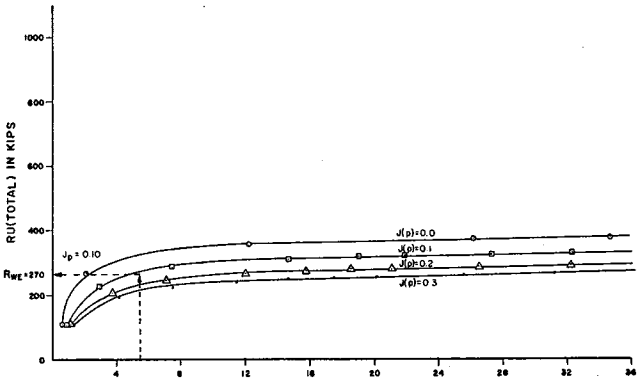

Fig. D.33. Blows/inch vs RU(total) for Muskegon Load Test Pile 9.